Chapter 14

Recognizing a Glaucomatous Optic Disc

Vassilis Kozobolis, Aristeidis Konstantinidis and Georgios Labiris

Additional information is available at the end of the chapter

http://dx.doi.org/10.5772/55157

1. Introduction

Glaucoma is an optic neuropathy with its hallmark being a characteristic loss of the ganglion cell axons which in turn leads to an excavation of the optic disc. Although optic disc cupping occurs in many other ocular diseases [1] the assessment of the optic nerve head with either optic disc photography or the newer modalities remains of utmost importance in the diagnosis and follow up of the glaucomatous process. The digital stereophotographs allow storage of optic disc photos for future comparison and offer qualitative assessment of the optic nerve head. The new imaging modalities can quantitatively and objectively analyze various parameters of the optic nerve head and the retinal nerve fiber layer in order to discriminate between glaucomatous and nonglaucomatous optic discs. They can also compare scans of the same patient overtime and detect any changes. As glaucoma is a progressive optic neuropathy patient's assessment overtime is of paramount importance in order to tract changes and monitor the progression of the disease.

1.1. New modalities for the imaging and analysis of the optic disc and retinal nerve fiber layer (RNFL)

1.1.1. Red-free photography of the optic disc and RNFL

Photography is not a new imaging technique [2,3]. However newer photographic methods allow stereographic assessment of the optic nerve head and more detailed visualization of the RNFL. Retinal nerve fiber layer is better visualized when the refractive media are clear and in pigmented fundi. Its defects can be broadly classified as localized and diffuse and the former are easier to identify.Red free photography of the RNFL is as accurate in distinguishing glaucomatous from nonglaucomatous patients as optical coherence tomography (OCT),

scanning laser polarimetry (SLP) and confocal scanning laser ophthalmoscope (SCLO) [4,5]. Stereophotographs of the optic discs was proven to be as efficacious in detecting glaucoma as the objective analysis the optic nerve head with the new modalities [6,7].

The new imaging modalities on the optic disc and RNFL include the confocal scanning laser ophthalmoscopy (CSLO), optical coherence tomography (OCT) and scanning laser polarimetry (SLP). The first two technologies can analyze both the optic nerve head and RNFL while SLP analyzes the thickness of the RNFL only.

1.1.2. Confocal Scanning Laser Ophthalmoscopy (CSLO, fig 1)

The CSLO technology is used by the Heidelberg Retinal Tomograph (HRT, Heidelberg Engineering, Heidelberg, Germany). It is based on the principle of two conjugated pinholes. Laser light (670nm) enters through one pinhole and focuses on a plane of the retina or the optic disc. The reflected light passes through the confocal pupil and allows reflected light only from that specific plane to enter the photodetector. The focused laser light scans across the optic nerve head (ONH) and RNFL along the x and y axes at planes of different depth acquiring a series of images. This series is reconstructed to produce a three dimensional image. Each series consists of 16 images per mm and for a 4 mm depth scan 64 images are captured. A fundamental part of the SCLO technology is the reference plane. It is defined as a plane parallel to the retina and lies 50 μm below the temporal part of the scleral ring of Elsching. In ONH analysis structures above the reference plane are read as neuroretinal ring and structures below are read as disc cup. SCLO has a transverse resolution of 10 μm and an axial resolution of 300 μm. The field of view of the image is 15°×15°.

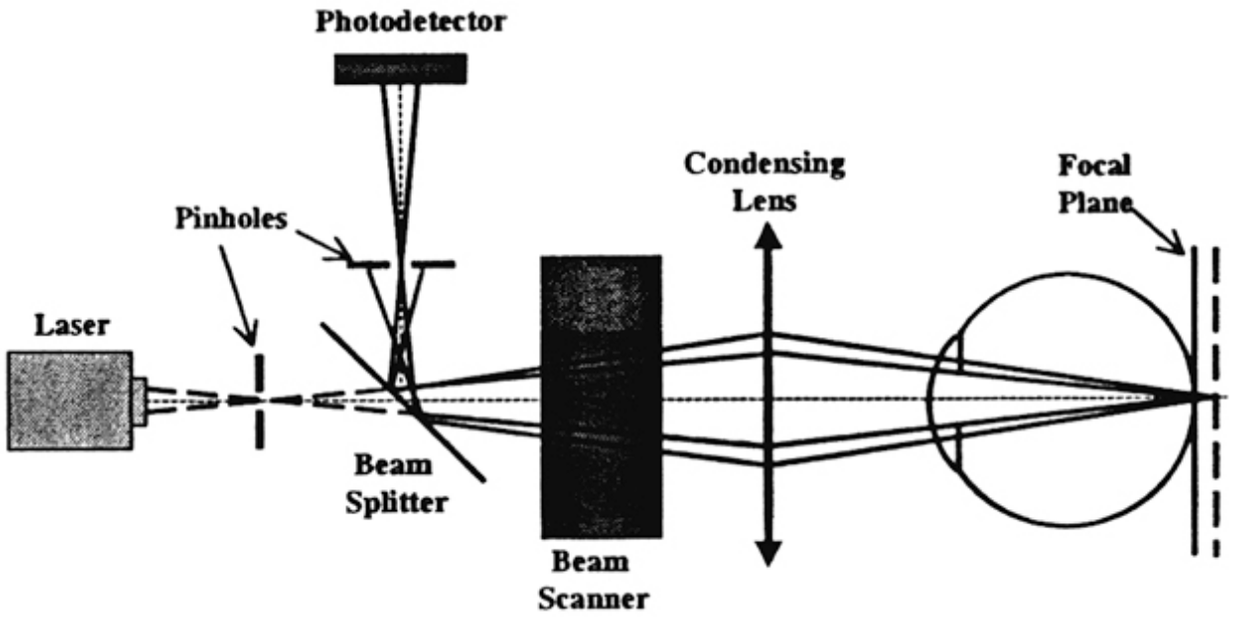

Figure 1. Light from the laser device passes through a pinhole sitting in front of it and focuses on a certain plane in the retina. The reflected light from the retina enters a confocal pinhole sitting in front of the photodetector. Only light

http://dx.doi.org/10.5772/55157

reflected from that specific plane (as determined by the position of the pinhole in front of the laser device) enters the photodetector. The focal plane can be changed by moving the pinhole of the laser device.

The HRT can analyze both the RNFL thickness and optic nerve head. A fundamental part of the analysis is the identification of the boundaries of the optic disc. The operator can draw a line along the edge of the optic disc. As the retinal vessels and peripapillary atrophy can make the exact identification of the boundaries difficult the examiner can use the 3-dimensional image of the optic nerve head in order to draw the line.

The RNFL thickness is measured at the edge of the optic nerve head for 360° and follows a double hump appearance as the RNFL is thicker in the superotemporal and inferotemporal sectors. The optic disc parameters analyzed are: the disc area, cup area, rim area, cup volume, rim volume, linear cup/disc ratio, mean cup depth. Mean cup depth, maximum cup depth, cup shape measure, height variation contour, mean RNFL thickness and RNFL cross-sectional area. The Moorfields regression analysis provides an overall assessment of the field of view and classifies it as "normal", "borderline" and "outside normal limits".

2. Strengths and limitations [8]

The advantages of the new version of CSLO (HRT 3) is the large normative database which includes subjects European, African and Indian ancestry and can analyze both optic nerve head and RNF. Its limitation is that some optic nerve head measurements rely on a reference plane based on a hand drown contour line around the disc margins. The Glaucoma Probability Score does not need a reference plane. HRT measurements can be influenced by intraocular pressure fluctuations [9].

2.1. Optical Coherence Tomography (OCT, fig 2)

Optical coherence tomography uses the principle of interferometry to construct high resolution cross-sectional images of the retina. An 800 nm laser light is split into two beams before entering the eye. The imaging beam consists of short pulses of light (the duration of each pulse is defined as the coherence length). One beam enters the eye and is reflected from the retina and the second beam is reflected from a reference mirror that moves back and forth along the Z axis. When the two reflected light beams constructively interfere they create a signal read by the interferometer. The time delay of the back scattered light from each layer of the retina differentiates the depth location of each layer (time-domain OCT). As a consequence in time domain OCT the instrument needs to perform two scans: a transverse scan across the eye (x axis) and a depth scan (z axis).The upgrade of time-domain OCT is the spectral-domain or Fourier-domain OCT (SD OCT/FD OCT). The SD OCT instead of the mechanical movement of the reference mirror analyzes with the aid of a mathematical equation (Fourier transform: $F_S(z) \propto FT\{A_S(K\}$) multiple wavelengths reflected from the retina. SD OCT obtains retina scans much faster (as the movement of the reference mirror along the z axis is omitted and only the scanning of the beam along the x axis is used) and with a better resolution (5-6 μm axial resolution, 10-15 μm transverse resolution) than the time-domain OCT. For the analysis of the

optic nerve head the OCT runs six scans across the optic disc in a spoke-like pattern (fig 3). The measurements of the area between the scans are interpolated from the values across the scans. The edge of the optic nerve head is automatically defined as the end of the retinal pigment epithelium (RPE)/choriocapillaris layer. A straight line is taken from one edge of the RPE to the other and a reference plane is set 150 μm above this line. Neuroretinal rim is defined as the area above the reference plane and cup the area below it.

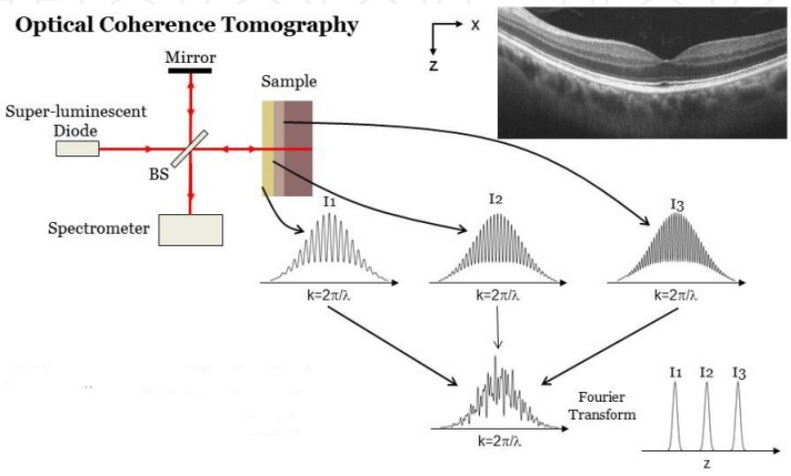

Figure 2. The beam from super-lumiscent diode laser source is split as it travels through the beam splitter (BS). One beam goes to the reference mirror (mirror) and the second beam in the tissue to be examined. The two beams are reflected back and they interfere as they enter the interfereometer (spectrometer in the figure). The mirror moves back and forth in order to create constructive interference at different depths (represented by different colors in the sample) of the examined tissue (z axis). The beam also travels across x axis in order to capture a slice of the sample.

3. Strengths and limitations [8]

OCT can analyze both the morphology of the optic disc and RNFL (fig 3,4). However automatic recognition of the edges of the optic disc as the end of the RPE layer can give incorrect measurements in patients with peripapillary atrophy. This is especially true for glaucoma patients who tend to have greater peripapillary atrophic areas that progress overtime. In this case what is incorrectly measured as optic disc area is the area of the optic nerve head plus the peripapillary atrophy. Furthermore as the information of the optic nerve head data between the scans are interpolated small defects of the neuroretinal rim may be missed.

3.1. Scanning Laser Polarimetry (SLP) (fig 5,6)

Scanning laser polarimetry is used in the GDx (GDX; Carl Zeis Meditec, Dublin, CA, USA). It is based on the principle of retardation. The RNFL has linear birefringence due to the parallel orientation of the microtubules in the axons of the RNFL. When polarized light travels through the RNFL the beam parallel to the RNFL slows down compared to the one that travels

http://dx.doi.org/10.5772/55157

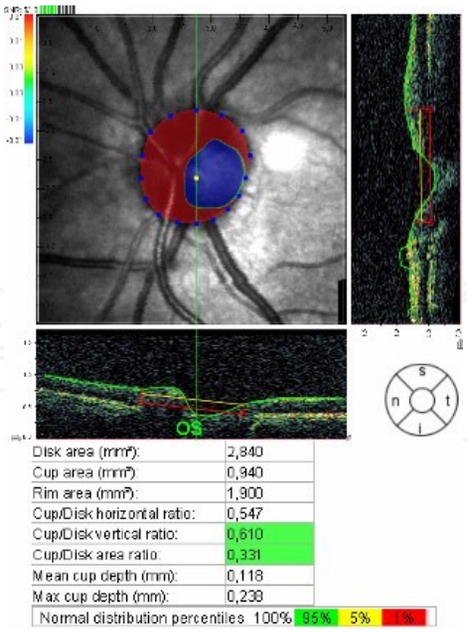

Figure 3. Optic nerve head analysis of a normal optic disc. The disc margins are identified by the OCT but the examiner can accurately identify the true disc border by manually moving the blue squares. The parameters measured are shown in the figure

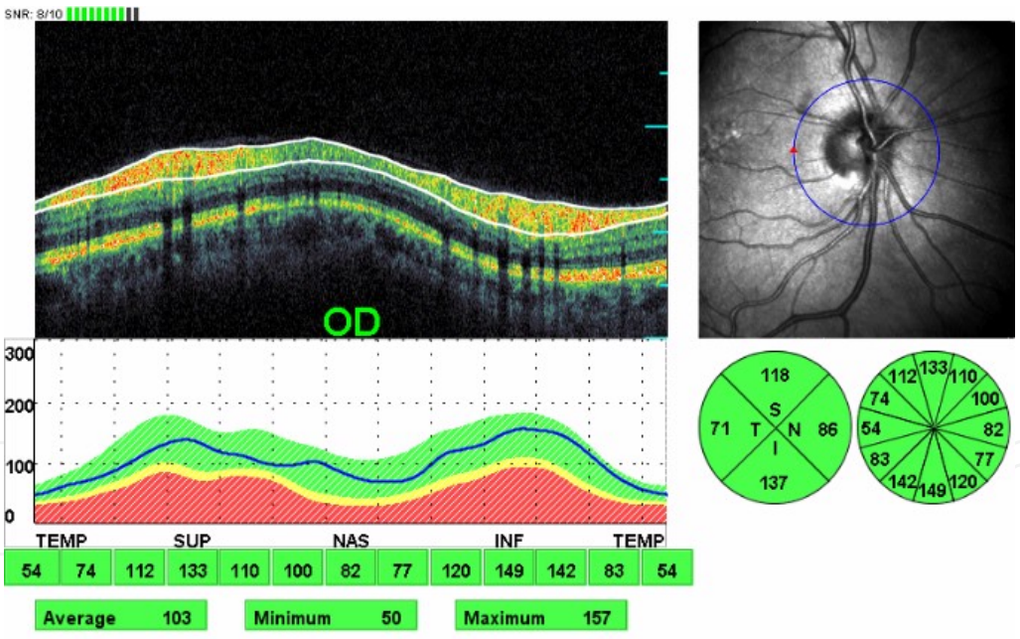

Figure 4. RNFL analysis with OCT. The numbers refer to RNFL thickness in µm. The green shaded area represents the normal RNFL thickness in the normative database of the OPKO spectral-domain OCT/SLO (Opko/OTI, Ophthalmic Technologies Inc, Toronto, Canada). Ninety five percent of the age-matched subjects with normal RNFL thickness will be included in the green area. On the other hand <5% of the subjects with normal RNFL thickness will fall in the yellow shaded area and <1% of the normal subjects will be in the red shaded area. In this patient the blue contour line of their RNFL thickness has the characteristic double hump appearance and falls in the green area. The RNFL thickness is normal for the age of this patient. The double hump pattern of the RNFL is due to the increased thickness of the fiber layer in the superotemporal and inferotemporal sector. The RNFL thickness is measured around a 3.46 mm diameter circle centered on the optic disc.

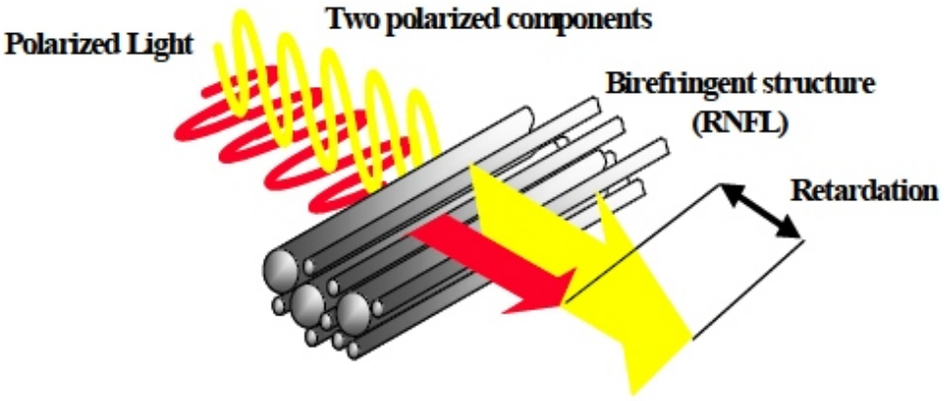

Figure 5. Polarized light that travels parallel to the RNFL slows down. This retardation is proportional to the thickness of the RNFL

perpendicular to the fiber layer. This difference in the speed between the two beams is called retardation and is proportional to the RNFL thickness. The scanning laser beam used is 785nm.

Because the corneal also exhibits birefringence the GDx has a variable corneal compensator (VCC) in order to subtract the retardation from the cornea and the only retardation measured is that derived from the RNFL. The newer GDx machines have an enhanced corneal compensator that offers better reproducibility of the measurements and is more accurate in the diagnosis of glaucoma [10]. The transverse resolution of the GDx is 45 μm.

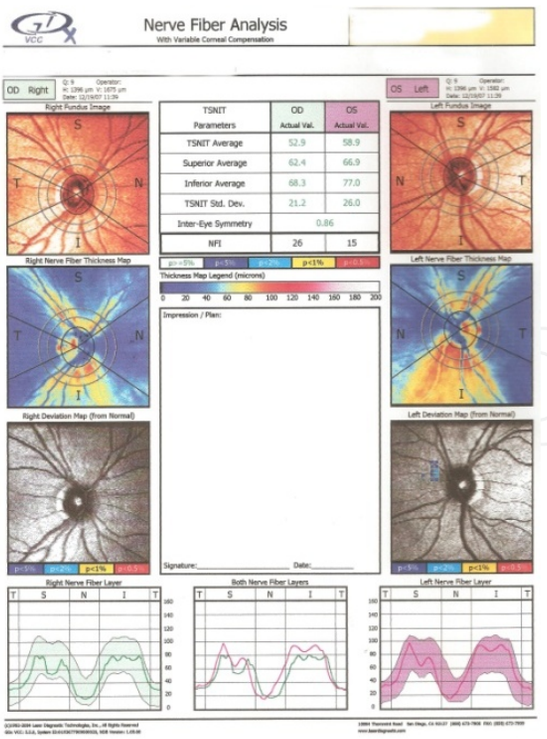

Figure 6. Printout of the RNFL analysis with the GDx VCC. The colored images at the top of the printout are the fundus photos. Below them is the thickness map. It is a color coded representation of the thickness of the RNFL within a 20° × 20°

http://dx.doi.org/10.5772/55157

(128×128 pixels) field centered on the optic disc. The warmer the colors the thicker the RNFL. Below the thickness map is the deviation map which represents the deviation of the RNFL thickness from the normal age matched value. At the bottom is the TSNIT (Temporal – Superior – Nasal – Inferior – Temporal) map which shows the RNFL thickness along the calculation ring. The latter is a ring 0.4 mm wide centered around the optic disc with the outer diameter being 3.2 mm and the inner 2.4 mm. The shaded areas (green for the right eye and purple for the left) represent the 95% of the normal values for this age group. The TSNIT contour line has a double hump appearance as for the OCT. The TSNIT parameters are the RNFL thickness along the calculation ring for the average, superior and inferior sector RNFL thickness. The TSNIT standard deviation is the modulation from peak to trough values of the double hump pattern. Because in glaucoma the superior and inferior sectors become thinned the difference between the peks and troughs decreases the TSNIT standard deviation value decreases as well. The intereye symmetry measures the symmetry between the eyes (values between -1 and 1). Normal eyes show good symmetry but the glaucomatous eyes tend to be asymmetrical as glaucoma can affect one eye more than the other. The Nerve Fiber Indicator is a global value based on the entire RNFL thickness map. The values range from 1-100 (1-30: normal, 31-50: borderline, >51: abnormal).

4. Strengths and limitations [7]

SLP can only measure data from RNFL. Areas of peripapillary atrophy give false information about the RNFL. A minority of the eyes examined show atypical retardation patterns (APRs) which are overcome by the GDx-ECC machines [11]. Atypical patterns are those which do not follow the normal histological distribution of the RNFL with the supero- and inferotemporal sectors being the thickest. APRs give falsely high RNFL measurements [12]. Newer SLP models are not compatible with the older ones. On the other hand RNFL analysis with SLP does not require a reference plane.

5. Sensitivity and specificity

Badala et al [4] compared the efficacy of stereoptic disc assessment and that of all three imaging modalities (OCT, GDx, HRT 3) in diagnosing glaucoma. The sensitivity at 95% specificity of the best performing parameter of each modality is: for the OCT (average RNFL thickness) 89%, for the GDx VCC (nerve fiber indicator) 78% and for the HRT 3 [Frederick S. Mikelberg (FSM) discriminant function] 70%. Optic disc stereophtographs are as accurate in detecting glaucoma as the other imaging modalities.

Retinal nerve fiber analysis with all the above modalities exhibit a characteristic double hump because the RNFL in thicker in the superotemporal and inferotemporal sectors compared to the nasal and temporal ones.

All of the above imaging modalities have been employed in the diagnosis and follow up of patients with various stages of glaucomatous optic neuropathy. Studies have shown that there is a discrepancy between the measurements of the optic disc parameters taken with OCT and HRT in glaucomatous eyes [13]. HRT II had higher values for disc and rim area while RTVue-100 OCT had higher values for cup area, cup-to-disc area ratio, and vertical and horizontal cup-to-disc ratio. Leite et al [14] compared three FD-OCT machines and reported that their performance in detecting glaucoma is similar. FD-OCT out-performed SD-OCT in detecting progression of the glaucomatous process [15] but they were comparable in detecting glaucomatous damage [16]. Lee et al [17] found that the best performing parameter for

glaucoma detection of the GDx is the nerve fiber index and that for Cirrus OCT the inferior RNFL thickness. GDx was also more accurate in detecting glaucoma than the Cirrus OCT. Two recent studies [18,19] showed that the diagnostic accuracy for glaucoma of the HRT II is dependent on the disc size which is not the case for OCT and GDx.

The severity of the glaucomatous process also affects the accuracy of glaucoma diagnosis of the various imaging technologies. The more advanced the disease the more accurate the diagnosis of glaucomatous optic neuropathy [20,21]. OCT and SLP performed better than CSLO in discriminating between early glaucomatous eyes with or without visual field defects [22]. In eyes with early glaucoma the most accurate parameter is the inferior RNFL thickness which performs better than the most accurate parameter of the CSLO (vertical cup-to-disc ratio). In glaucoma suspect eyes the most accurate parameter for the OCT is the average RNFL thickness, for the SLP the nerve fiber indicator and for the CSLO the vertical cup-to-disc ratio. The first two parameters performed better than the vertical cup-to-disc ratio. Leung et al [23] confirmed that SD-OCT performed better than HRT in recognizing patients with glaucoma. RNFL thickness changes performed better than optic nerve head parameters as evaluated with CSLO. The nerve fiber index of the SLP was more accurate in diagnosing glaucoma than the rim volume parameter of the CSLO [24]. SLP was also superior in detecting glaucoma progression by analyzing RNFL thickness compared to CSLO analysis of the neuroretinal rim area [25].

6. Anatomy of the optic disc (fig 7)

The optic disc is the area in the posterior pole where the ganglion cell axons converge to exit the eye and travel towards the brain. Its margins are defined by a dense fibrous tissue, the Elsching's ring. The disc area is covered by the neuroretinal rim which contains the retinal ganglion cells axons and the disc cup in the center. The ganglion cells axons leave the eye by piercing the thinned part of the sclera called the lamina cribrosa. The axons are arranged in bundles and exit the eye via the pores of the lamina cribrosa to form the optic nerves. The size and shape of the neuroretinal rim and cup depend on the total size of the optic disc and the number of the axons that travel through it.

The following morphological features of the optic disc should be taken into account when assessing an optic nerve head [26]:

6.1. Optic disc size

The size of the optic disc shows great variability between different populations [27]. The range of the mean disc area measured in mm^2 for people of different ethnic backgrounds is: africans 1.84-2.50, whites 1.65-2.34, Indians 2.24-2.93, Asians 1.97-2.67 and latinos 1.95-2.56 [28].The size was shown to be independent of the age after the age of 10, the body height, gender and refractive errors between -5.00 and +5.00 D. In contrast the optic disc is smaller in high hypermetropes and larger in high myopes. Optic disc size abruptly increases for myopia above -8.00 diopters (D) and significantly decreases for hyperopia above +4.00 D [29] The optic disc area was found to have great variability between healthy individuals by many researchers [28,30,31]. For this reason the terms <<microdisc>> and <<macrodisc>> have been coined.

http://dx.doi.org/10.5772/55157

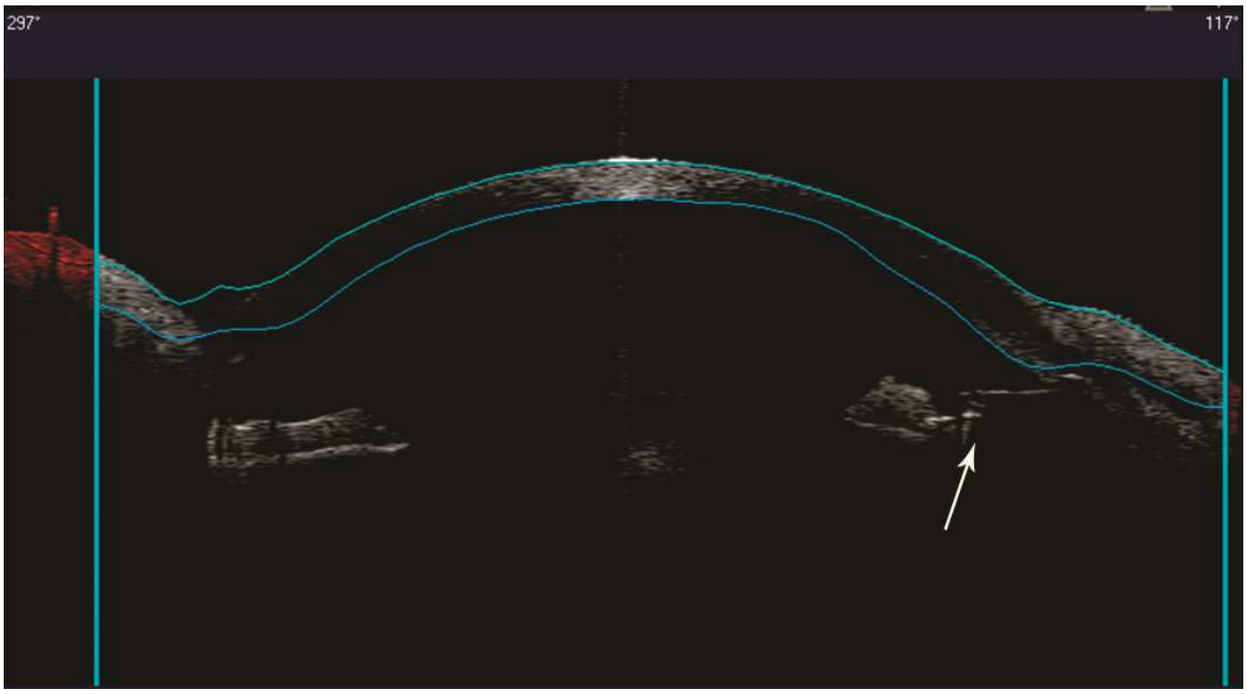

Figure 7. Normal optic disc. Note the presence of a small cup, thick neuroretinal rim, absence of peripapillary atrophy, equal distance of the exit of the trunk of the vessel from the superior and inferior sectors of the rim and normal arteriolar caliber.

Microdisc is a disc with a disc area two standard deviations less than the mean of the normal disc area and macrodisc is a disc with a disc area two standard deviations above the mean. The Blue Mountain Study [32] classified the discs as small (1.1 – 1.3), medium (1.4 – 1.7) and large (1.8 – 2.0) based on the vertical disc diameter measured in mm. The European Glaucoma Society classified the disc based on the disc area as small (<1.6mm^2), medium (1,6-2.8 mm^2) and large (>2.8 mm^2). Patients with primary open angle (POAG) and pigmentary glaucoma have normal disc size. In non-glaucomatous pathologies, optic disc drusen, pseudopapilledema, nonarteretic anterior ischemic optic neuropathy and tilted disc [33] are associated with small disc sizes while morning glory syndrome and optic disc pits with large discs. Furthermore larger discs have more axons in absolute number but less axons per disc area [34]. Patients with pseudoexfoliation glaucoma tend to have smaller discs and those with normal tension glaucoma larger discs [35,36]. Glaucoma, however, may occur in conjunction with abnormal disc size as well as with other disc pathologies.

6.2. Optic disc shape [26]

The optic disc is elongated along the vertical axis with the vertical axis being 7-10% longer than the horizontal. The disc shape as expressed by the ratio of minimal to maximal diameter shows less variability between individuals than the disc area. The disc shape is independent from sex, age, right and left eye and body weight and height and does not show interindividual variability for a refractive error less than -8.00D. In POAG patients the disc shape is not associated with the visual field defects. However for in high myopes >-12D it is more elongated.

Elongated optic discs were associated with increased corneal astigmatism. Overall disc shape bears little value in the diagnosis of glaucoma.

6.3. Neuroretinal rim shape and cup-to-disc ratio (C/D ratio)

It represents the quotient of the vertical cup diameter to the vertical overall disc diameter. In normal eyes the cup is horizontally elongated with the horizontal diameter being 8% longer than the vertical one. On the other hand the disc is vertically oval shaped. As a consequence the neuroretinal rim is thicker at superior and inferior poles. The mnemonic ISNT rule dictates that the neuroretinal rim is thicker in the inferior pole of the disc followed by the superior, the nasal and finally the temporal which is the thinnest. The C/D ratio also shows interindividual variability being higher in large discs and lower in smaller discs. Clinicians should bear in mind the opposite configuration of the cup and optic disc when assessing the disc for glaucomatous damage. They should also take into account that a high C/D ratio is not necessarily pathognomonic for glaucoma as it can occur in large diameter discs (fig 8,9). Conversely early glaucomatous damage can be overlooked in small discs with small cups.

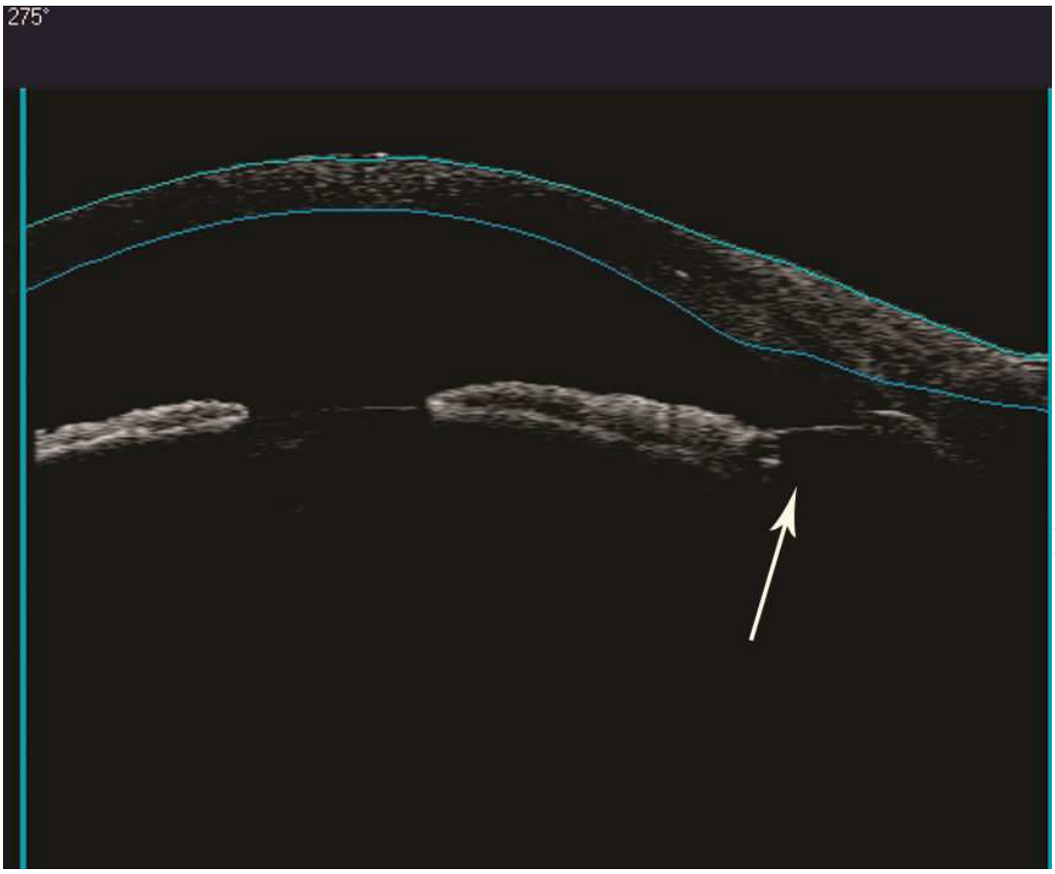

Figure 8. Large optic disc with a large cup. Neuroretinal rim shape respects **ISNT** rule (rim sectors wider to thinner (**I**nferior-**S**uperior-**N**asal-**T**emporal), there is no peripapillary atrophy and no optic disc haemorrhages are detected. The main vessels emerge with a dual trunk. The exit of each trunk lies at equal distance from the superior and inferior rim

http://dx.doi.org/10.5772/55157

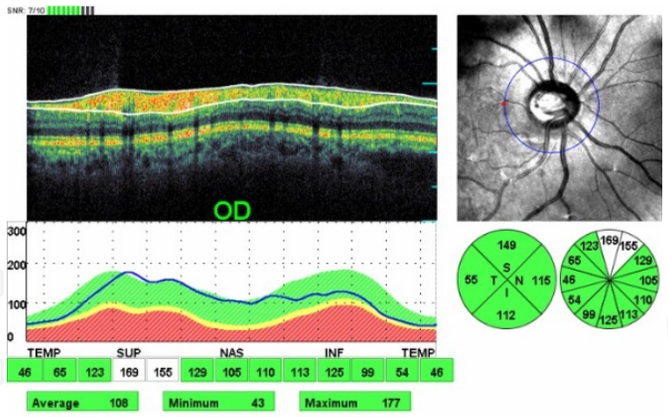

Figure 9. Retinal nerve fiber analysis (RNFL) with optical coherence tomography (OCT) of the same eye as in fig 8. The blue contour line represents the thickness of the RNFL of this patient and falls in the falls area. It is normal for this patient's age

In the early to moderate glaucoma the axons in the superotemporal and inferotemporal areas of the disc are affected usually first and this leads to an increase of the C/D vertical diameter faster than the horizontal causing an increased vertical C/D ratio with violation of the ISNT rule.

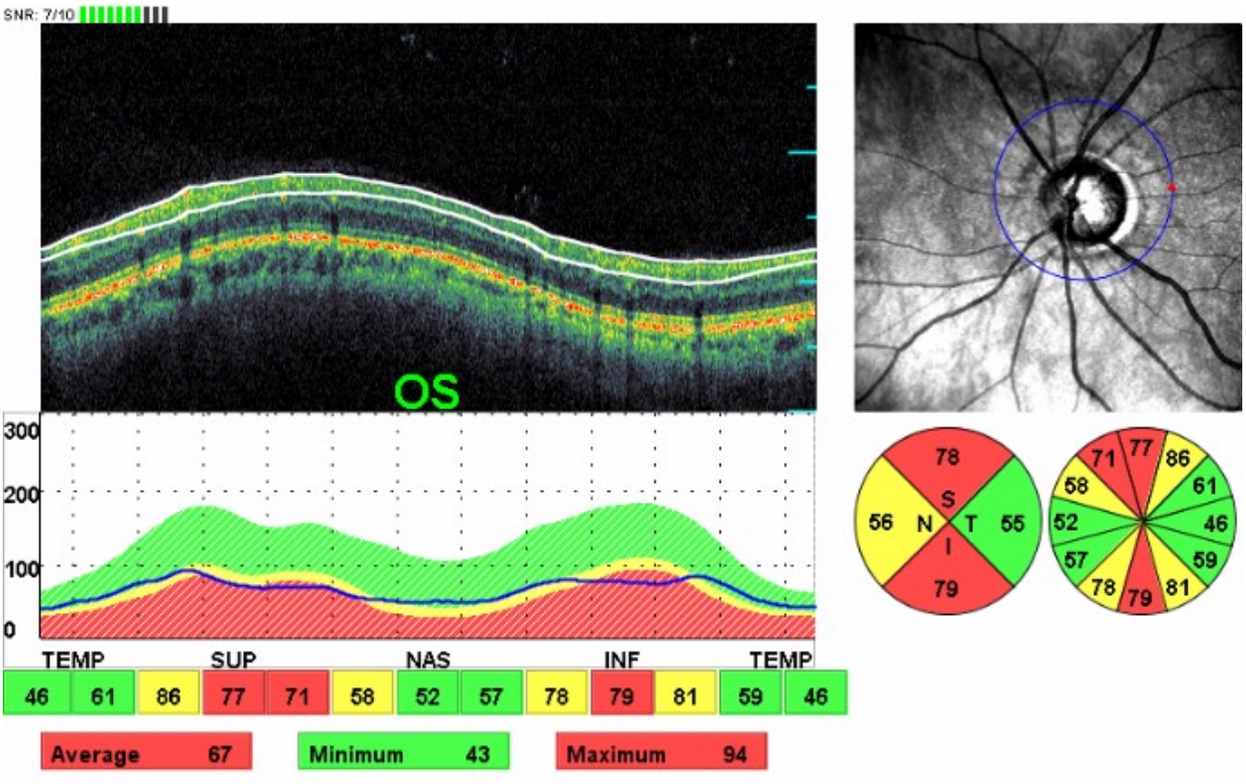

Figure 10. Typical RNFL loss in the superior and inferior RNFL sectors in a glaucoma patient. The RNFL contour line is flattened and crosses the red shaded abnormal area. Less than 1% of the normal subjects will have a similar RNFL thickness in the affected sectors as this patient has.

A large C/D ratio has been shown to be a risk factor for glaucoma progression [37], although Cioffi et al argued that it merely represents undetected damage [38].

6.4. Retinal Nerve Fiber Layer (RNFL)

The retinal nerve fiber layer is made up of the nonmyelinated axons of the retinal ganglion cells. They are more visible in the inferotemporal and superotemporal areas of the fundus and least visible in the horizontal nasal and temporal sectors. The visibility of the RNFL corresponds to the configuration of the neuroretinal rim which is thicker in the superior and inferior poles of the disc [26] giving a double hump configuration in the OCT RNFL analysis (fig 4). Defects in RNFL precede optic disc cupping in the corresponding sectors [39] as well as visual field defects with standard automated perimetry [40]. The most common sectors affected in glaucoma are the inferotemporal followed by the superotemporal [41]. This pattern of RNFL loss leads to the disappearance of the double hump configuration of the RNFL (fig 10,11). Nerve fiber defects are encountered in other optic nerve diseases such as optic disc drusen, toxoplasmic retinochoroidal scars, diabetic retinopathy and optic neuritis secondary to multiple sclerosis [26,42].

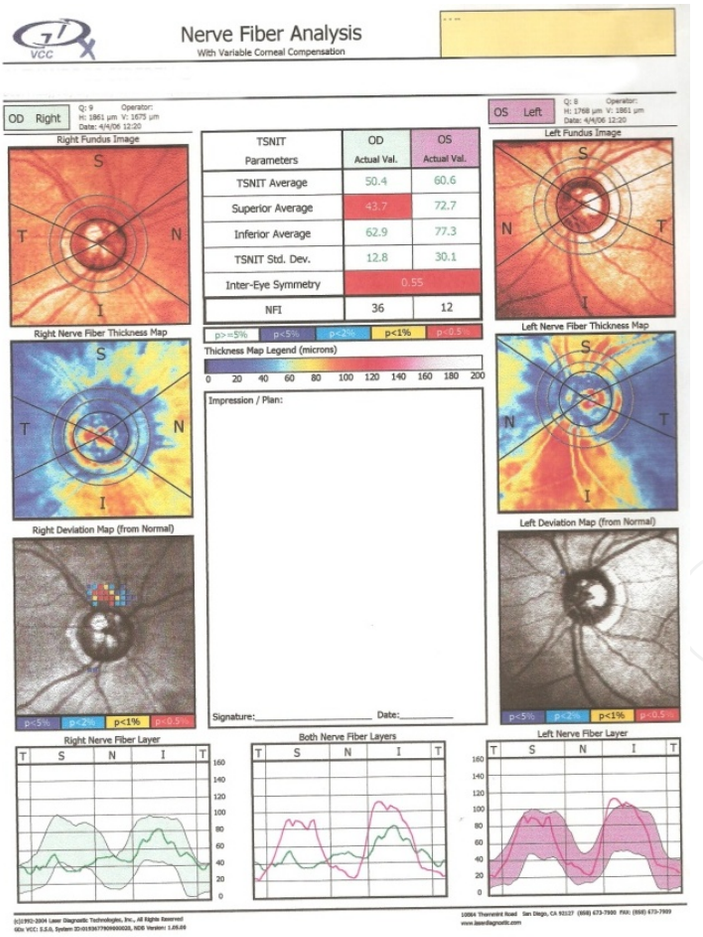

Figure 11. Thinning of the superior sector of the RNFL of the right eye due to glaucoma. Note the probabolity of each soperpixel (each superpixel includes 4 pixels) of the deviation to be normal. The purple pixel represent a 5% probability that the RNFL thickness in that superpixel is normal, the blue color represents a <2% probability, yellow <1% and

http://dx.doi.org/10.5772/55157

red <0.5%. The TSNIT map of the right eye has lost the double hump appearance, there is high inter-eye asymmetry as the left eye has not been affected by glaucoma and the NFI is high in the right eye.

6.5. Point of exit of the large vessel trunk on the optic disc

Research has shown that the area on the optic disc most susceptible to glaucomatous damage is the area that is the furthest away from the main vessel trunk (fig 12) [43]. The exit of the main vessel trunk is usually displaced superonasally which makes the inferotemporal quadrant more susceptible to the glaucomatous damage. The disc arterioles follow the contour of the neuroretinal rim. As the rim recedes in the glaucomatous process the arterioles tend to become displaced towards the periphery of the optic disc. If the rim becomes extremely thin the vessels may be pushed to the far periphery of the disc just next to the Elsching's ring and then they sharply angle on the retinal surface giving rise to the bayoneting sign (fig 13). The presence of a temporal cilioretinal artery has a protective role against the glaucomatous process [44]

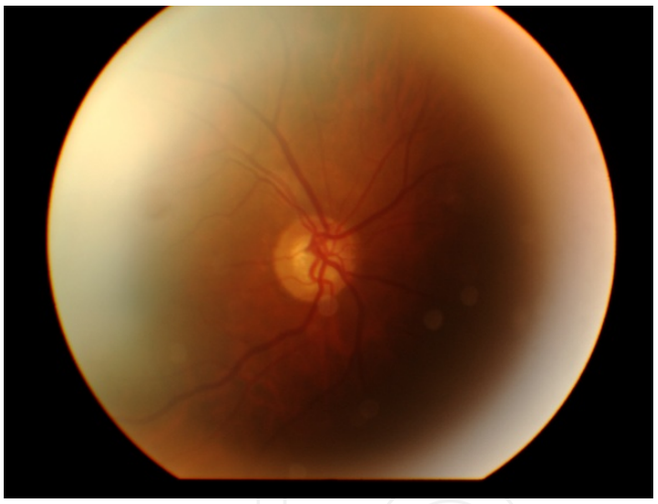

Figure 12. Right optic disc: The main vessel trunk emerges in the superotemporal disc quadrant. The neuroretinal rim is thinnest in inferior and nasal quadrants. The distance of the main vessel trunk to the inferior rim is longer compared to the distance to the superior rim. The glaucomatous damage is greatest in the inferior rim. There is no arteriolar narrowing

6.6. Optic disc haemorrhages (fig 14)

Optic disc haemorrhages are an independent risk factor for glaucoma and ocular hypertensive patients with disc haemorrhages are six times more likely to develop glaucoma than those patients without haemorrhages [45]. The frequency of disc haemorrhages in glaucoma eyes ranged from 9-20% [46,47]. Their frequency is not statistically different in glaucoma eyes with high or normal IOP [46]. Their prevalence in non-glaucomatous eyes ranges from 0.2% - 1.03% [48-51]

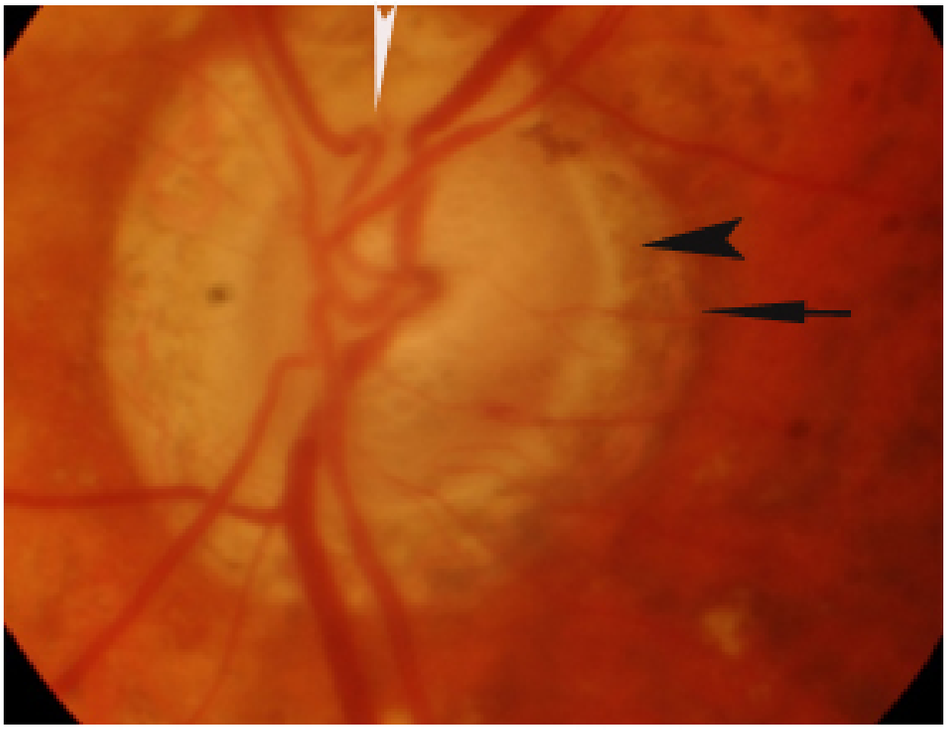

Figure 13. Large PPCA in advanced glaucoma with small alpha zone temporally (arrow) and a large beta zone (arrowhead). Bayoneting of the arterioles (white arrowhead)

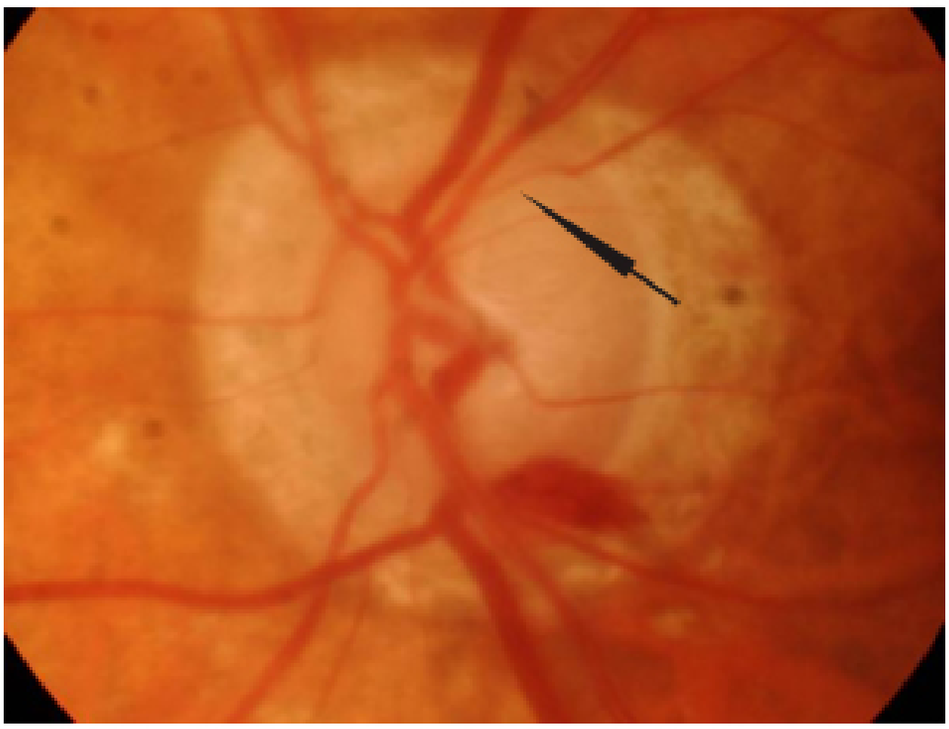

Figure 14. Optic disc haemorrhage in advanced glaucoma. Note the presence of focal arteriolar narrowing (arrow).

6.7. Peripapillary Chorioretinal Atrophy (PPCA, fig 13)

Peripapillary atrophy consists of an outer alpha zone with irregular hyper- hypopigmentation and an inner beta zone with visible large choroidal vessels and sclera. Alpha zone is present in most normal eyes but beta zone is more common in glaucoma eyes and tends to enlarge in eyes with progressing normal tension glaucoma [52]. They both tend to increase in size with advancing glaucoma damage [53]. The frequency of the beta zone varies between 59.5% and 69% in glaucoma patients and 17.4% and 24% in healthy subjects [53,54]. Beta zone is also larger in glaucomatous eyes (1.21 ± 1.92 mm ^{2}) compared to healthy ones (0.32 ± 0.99 mm^2) [54]. There is conflicting evidence as to whether the PPCA corresponds to areas of neuroretinal rim thinning. Uchida et al [55] reported that PPCA progression correlated to progressive disc damage and visual field defects. On the other hand See et al [56] showed that neuroretinal area decrease did not correlate with PPCA progression. The extent of PPCA positively correlated with the presence of optic disc haemorrhage in glaucoma eyes [57]. In this study beta zone was larger in the eyes with disc haemorrhage.

6.8. Retinal arterioles diameter

The diameter of retinal arterioles is decreased in both glaucomatous and non-glaucomatous optic nerve damage (fig 14). It merely represents the limited needs of the retina for oxygen rather the cause of the optic nerve damage [26]

7. Glaucomatous versus non-glaucomatous damage

Optic disc cupping is not pathognomonic for the glaucomatous optic neuropathy only [58]. Other diseases such as arteritic ischemic optic neuropathy (AION), optic neuritis, optic disc pit, colobomas, tilted disc, traumatic optic neuropathy, methanol toxicity, compressive lesions of the anterior visual pathways [59], disc drusen, long standing papilledema [26]. However nonglaucomatous disc damage produces optic disc rim pallor while glaucomatous damage produces focal or diffuse obliteration of the neuroretinal rim [60]. Glaucoma damage tends to produce deeper cups than the nonglaucomatous type [61]. In this study open angle glaucoma eyes had larger and deeper cups and smaller neuretinal rims compared to eyes with nonarteritic and arteritic AION. Contrary to glaucoma PPCA does not increase in nonglaucomatous damage [62].

Summary box

There is great variability among healthy subjects and people from different races in the morphology of the optic disc which makes the diagnosis of glaucoma very complicated. The clinician should take into consideration various aspects of the anatomy of the optic nerve head and the RNFL before deciding whether a patient has glaucoma or not

---

8. Congenital anomalies of the optic disc

8.1. Tilted disc

The tilted optic disc syndrome is caused by an oblique insertion of the optic nerves in the globe usually inferonasally. Its prevalence is around 0.5% and is commonly bilateral. It is associated with high myopia, astigmatism, visual field defects (usually superotemporal arcuate scotomas), small optic disc area, low best corrected visual acuity, peripapillary atrophy and choroidal neovascular membrane [63].

Tilted disc analysis with optical coherence tomography (OCT) showed decreased nerve fiber thickness of the superior, inferior and nasal sectors as well as on average, a thicker temporal sector and a more temporally positioned inferior and superior peak sectors (fig 15) [64]. Multifocal electroretinogram also revealed suboptimal macular function [65]

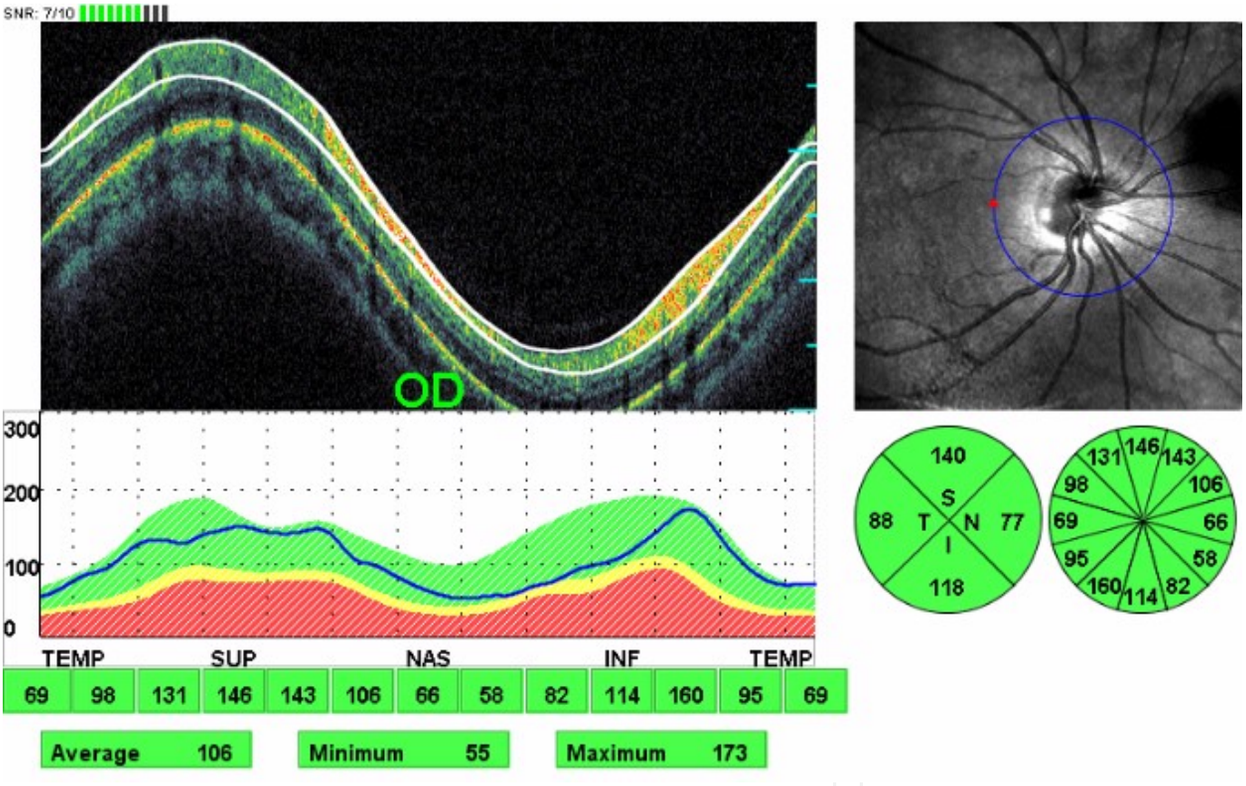

Figure 15. RNFL analysis with OCT in a patient with tilted disc. Slight thinning of the RNFL of the inferonasal sector. This patient has normal visual fields

8.2. Optic disc pit (fig 16)

Optic disc pits can be congenital or acquired. The former are a rare anomaly with a prevalence of 1:11,000 [66] and are associated with serous detachment of the macula which affects the vision and it can be treated with vitrectomy and gas tamponade. The acquired type is seen more often in pathological myopia and open angle glaucoma [67,68]. Their overall prevalence

http://dx.doi.org/10.5772/55157

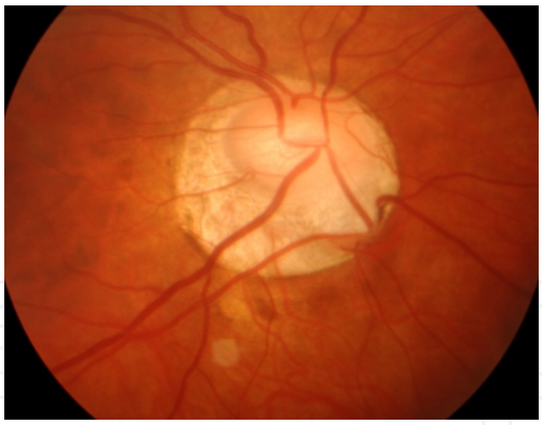

Figure 16. Peripapillary inferiorly located optic disc pit in a patient with primary open angle glaucoma.

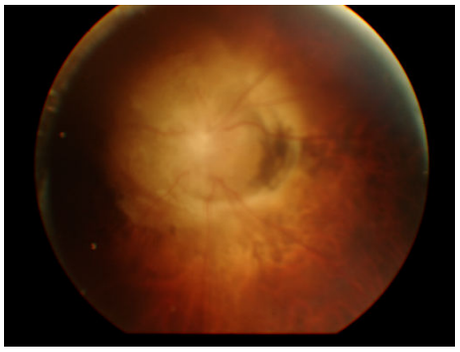

Figure 17. Morning glory syndrome. Visual acuity of this eye is hand movements with the other eye having similar clinical picture. The patient is registered blind.

in Blue Mountain Study is 0.19% [69]. The presence of optic disc pit in eyes with open angle glaucoma is a risk factor for progressive optic nerve head damage, advancing visual field defects and presence of disc haemorrhages. They more commonly seen in normal tension glaucoma than POAG and are associated with visual field defects close to fixation [70]

8.3. Morning glory syndrome (fig 17,18)

Morning glory syndrome is a rare developmental abnormality of the optic nerve. It is usually unilateral and can be complicated by serous retinal detachmant and choroidal neovascularization. The OCT analysis of the RNFL shows large optic discs, increased thickness of the RNFL and decreased macular thickness [71]. Morning glory syndrome is associated with systemic diseases such as frontonasal dysplasia, neurofibromatosis 2 and PHACE (Posterior fossa abnormalities and other structural brain abnormalities -

Hemangioma(s) of the cervical facial region - Arterial cerebrovascular anomalies, Cardiac defects, aortic coarctation and other aortic abnormalities - Eye anomalies) syndrome

8.4. Optic disc colobomas

This disc anomaly results from incomplete closure of the embryonic fissure and it is usually unilateral. Possible ophthalmic complications include serous macular detachment, optic disc excavation despite normal IOP and choroidal neovascularization. It is also associated with multiple syndromes such as Patau, Edwards and cat eye syndromes and **CHARGE** (**C**oloboma of the eye - **H**eart defects - **A**tresia of the choanae - **R**etardation of growth and/or development - **G**enital and/or urinary abnormalitie - **E**ar abnormalities and deafness) syndrome. In uncomplicated cases (without serous macular detachment) OCT analysis of the RNFL shows normal fiber layer thickness [72]

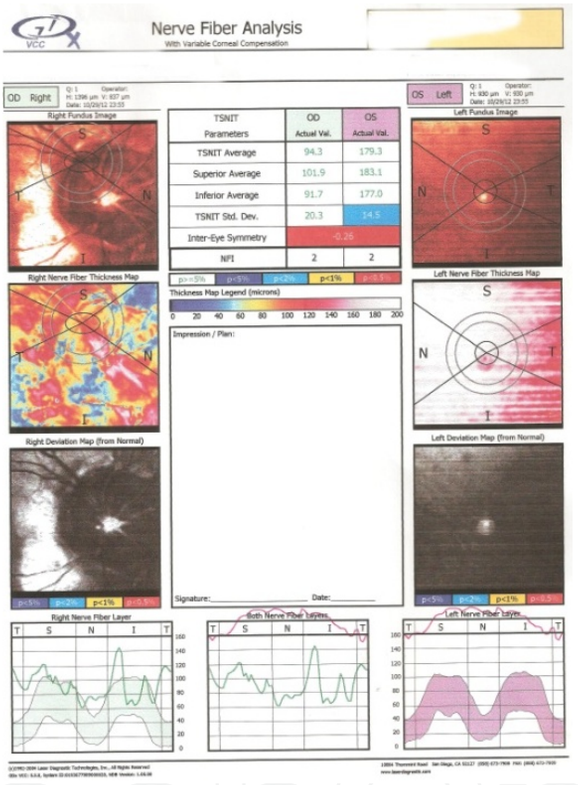

Figure 18. GDx VCC of the patient in fig 17. Note that the calculation ring is smaller than the optic nerve head and a meaningful analysis of the RNFL in this patient is not possible. The quality of the scan is poor due to nystagmus

8.5. Optic disc drusen

Optic disc drusen are hyaline bodies in the optic disc substance. Their prevalence is 3.4 – 24 per 1,000 and areusually bilateral [73]. They are usually located most commonly nasally and are difficult to visualize in childhood as they are buried but become more obvious in adolescence. Ophthalmic complications include choroidal and disc neovascularization and visual field defects. Disc drusen when buried can pose a diagnostic dilemma with papilledema. Disc drusen can be detected by fundus autofluorescence, B scan ultrasonography, computed tomography and recently OCT. Optical coherence tomography scans through the optic nerve

head can directly show the drusen. Lee et al [74] reported that the RNFL thickness with spectral domain OCT was increased in all sectors in patients with papilledema as opposed to optic disc drusen in which the RNFL was thicker in the temporal quadrants compared to normal subjects. This can be explained by either a mechanical displacement of the retinal fibers by the drusen which usually lie in the nasal sector towards the temporal sectors or by the compression and subsequent atrophy of the nasal retinal fibers. In longstanding papilledema the retinal fibers are damaged and the average RNFL thickness is reduced. Disc drusen appear hyporeflective on OCT scans [75].

8.6. Optic nerve hypoplasia

Optic nerve hypoplasia is a congenital disorder that can be uni- or bilateral, segmental or total and the visual acuity can be normal or reduced to no light perception. It can be associated with many syndromes with the most common being de Morsier syndrome.

Two studies [76,77] found that in patients with superior segmental optic hypoplasia is associated with generalized reduction of the RNFL thickness involving all the sectors and not only the superior one.

9. Acquired optic disc disorders

9.1. Papilledema

Papilledema is the bilateral disc swelling secondary to increased intracranial pressure. Although bilateral it may be asymmetrical. It can be caused by space occupying lesions in the cavity of the skull, idiopathic intracranial hypertension, obstruction of the ventricles, impaired cerebrospinal fluid adsorption by the arachnoid villi, severe systemic hypertension, cerebral venous thrombosis, diffuse cerebral oedema following trauma.

Differential diagnosis includes: malignant hypertension, bilateral optic neuritis with optic nerve head involvement (papillitis), bilateral anterior ischemic optic neuropathy, diabetic papillopathy, Leber's hereditary optic neuropathy, pseudopapilledema (optic disc drusen, hypermetropia), and toxic optic neuropathy.

Optical coherence tomography is helpful in diagnosing early papilledema. Vartin et al [78] found that the peripapillary total retinal thickness rather than the conventionally calculated RNFL thickness as measured with spectral domain OCT differentiated early papilledema from normal subjects. Peripapillary total retinal thickness as a diagnostic tool for subtle papilledema was also reported by Skau et al [79]. OCT is useful in the follow up of patients with papilledema. Rebolleda et al [80] followed up patients with papilledema for 12 months following presentation and found that RNFL thickness decreased with time and visual field defects improved. Kupersmith et al [81] investigated different causes of optic disc swelling [papilledema, non-arteritic anterior ischemic optic neuropathy (NA-AION) and optic neuritis] with OCT and scanning laser polarimetry (SLP). Retinal nerve fiber thickness by OCT was increased in papilledema and NA-AION compared to eyes suffering from optic neuritis. This is due to

greater disc edema in eyes with papilledema and NA-AION. SLP showed increased RNFL thickness in papilledema and optic neuritis. The authors concluded that OCT reveals increased retinal thickness due to axonal swelling but SLP shows the true damage of the axons.

Two studies investigated the morphology of the retinal pigment epithelium/Bruch's membrane (RPE/BM) complex and concluded that papilledema causes an inward (towards the vitreous cavity) bowing of the PRE/BM complex as opposed to patients with AION and optic neuritis [82,83]. The authors speculate that the increased pressure in the cerebrospinal fluid (CSF) caused the forward bowing of the RPE/BM complex. In the other types of disc swelling (AION, optic neuritis) pathophysiologically there is no high pressure of the CSF.

9.2. Optic Neuritis (ON) (fig 19)

Optic neuritis is the inflammatory process of the optic nerve. Anatomically it can affect the optic nerve head (papillitis), only the posterior part of the nerve (retrobulbar neuritis) or both.

Differential diagnosis includes: anterior ischemic optic neuropathy, compressive lesions of the optic nerve, Leber's hereditary optic neuropathy, central retinal vein occlusion, infiltration of the optic nerve head (sarcoidosis, tuberculosis, syphilis, leukemia)

Optical coherence tomography has been used in the diagnosis and follow up of patients with isolated optic neuritis or optic neuritis in clinically diagnosed multiple sclerosis (MS). It was found that as expected the patients with previous history of ON had thinner RNFL than normal subjects [84,85]. OCT can also demonstrate structural damage more accurately than standard automated perimetry. Noval et al reported that OCT can detect subtle RNFL changes in the presence of normal visual fields [86]. Interestingly Pro et al described RNFL thickening in the acute phase of ON even in patients without disc swelling [87]. OCT has been used in the follow up of patients with ON over time. Costello et al reported that the RNFL loss is more profound between the third and sixth month after the episode of ON [88]. The earliest damage in the RNFL is evident 2 months after clinical presentation and the RNFL damage halts 7 months after the episode of ON [89,90]. In patients suffering from multiple sclerosis, eyes unaffected by ON demonstrate lower RNFL thickness compared to normal subjects [91-95]. OCT findings have also been linked to visual function. Average RNFL thickness of less than 75μm predicted persistent visual dysfunction (90) and for every 1 line of reduced contrast sensitivity the RNFL thickness decreased by 4μm (91).

Secondary progressive MS was associated with greater RNFL decrease in both affected and unaffected by ON eyes (90, 92). Decreased RNFL thickness was also inversely associated with disease severity (the lower the RNFL thickness the more serious the disease) (95-97). Retinal nerve fiber thickness on OCT could not predict the risk of MS (96). In one study comparing the structural damage after optic neuritis it was found that only the modalities that measure RNFL thickness (OCT, GDx) were affected compared to disease free participants but the analysis of the optic disc with the HRT 3 was not statistically different compared to normal control group (99).

http://dx.doi.org/10.5772/55157

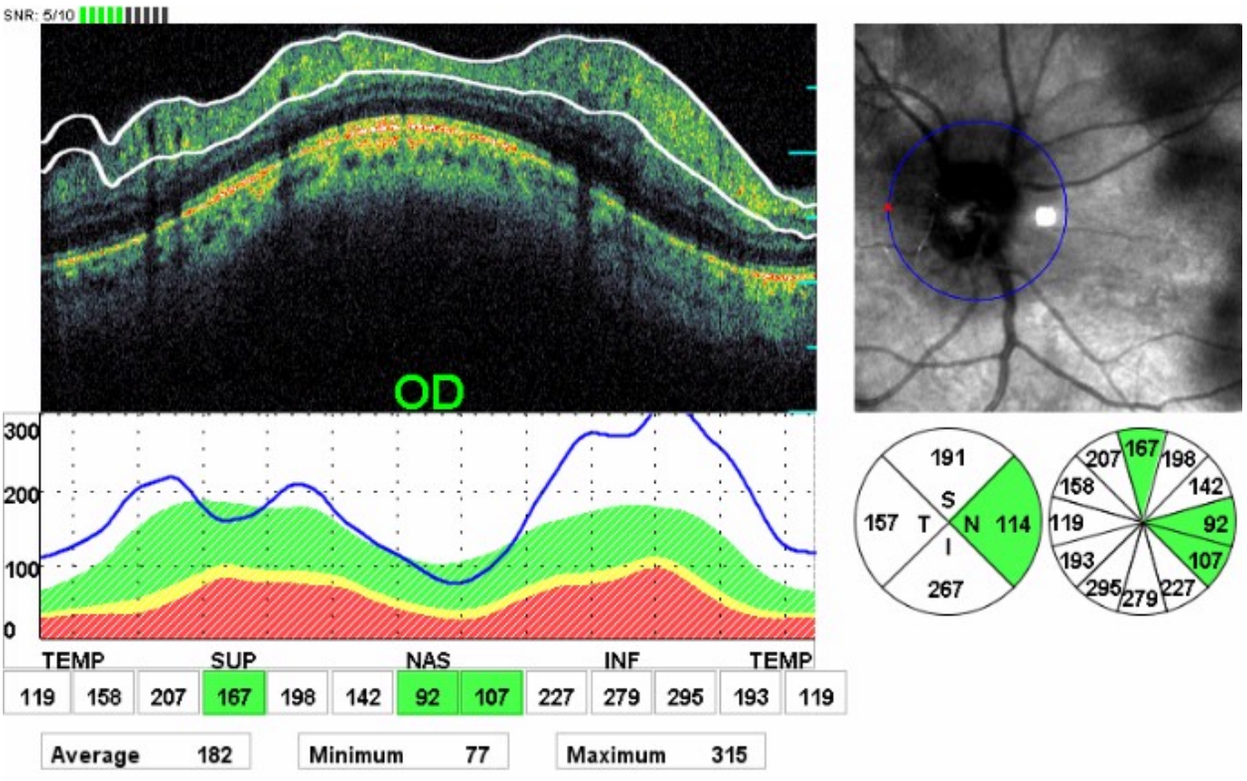

Figure 19. Swollen RNFL in a patient with papillitis secondary to multiple sclerosis.

9.3. Ischaemic optic neuropathy

Anatomically is classified as anterior and posterior and aetiologically as non-arteritic and arteritic. Predisposing factors for the non-arteritic anterior ischaemic optic neuropathy (NA-AION) is hypertension, diabetes mellitus, hyperlipidemia, sleep apnea, cataract surgery, erectile dysfunction, small crowded optic disc and long standing papilledema, while arteritic anterior ischaemic optic neuropathy (A-AION) is caused by giant cell arteritis. Posterior ischaemic optic neuropathy involves the retrolaminal part of the optic nerve. It can follow a heart or spine operation or be caused by giant cell arteritis or present as the posterior equivalent of non-arteritic AION. Differential diagnosis is as in optic neuritis.

Optical coherence tomography in the acute stages of AION shows diffuse thickening of the RNFL which turns into thinning as the disease becomes chronic (100,101) (fig. 20,21,22). Contreras et al (102) found that the superior RNFL quadrant was more affected and that for every 1μm of nerve fiber thickness loss there was 1 dB decrease of mean deviation in standard automated perimetry. OCT analysis of the RNFL showed RNFL thinning compared to healthy controls and the area of retinal axon loss correlated well with visual field defects (102-105). Macular thickness also correlated with visual field loss in eyes with NA-AION (106).

Research has shown that that AION and glaucoma affect the optic nerve differently. RNFL thickness in glaucoma and NA-AION eyes is not statistically different but it is markedly thinner compared to normal eyes (61,107). However when adjusting for mean deviation (MD) of visual fields RNFL was thicker in eyes with A-AION and NA-AION compared to open angle

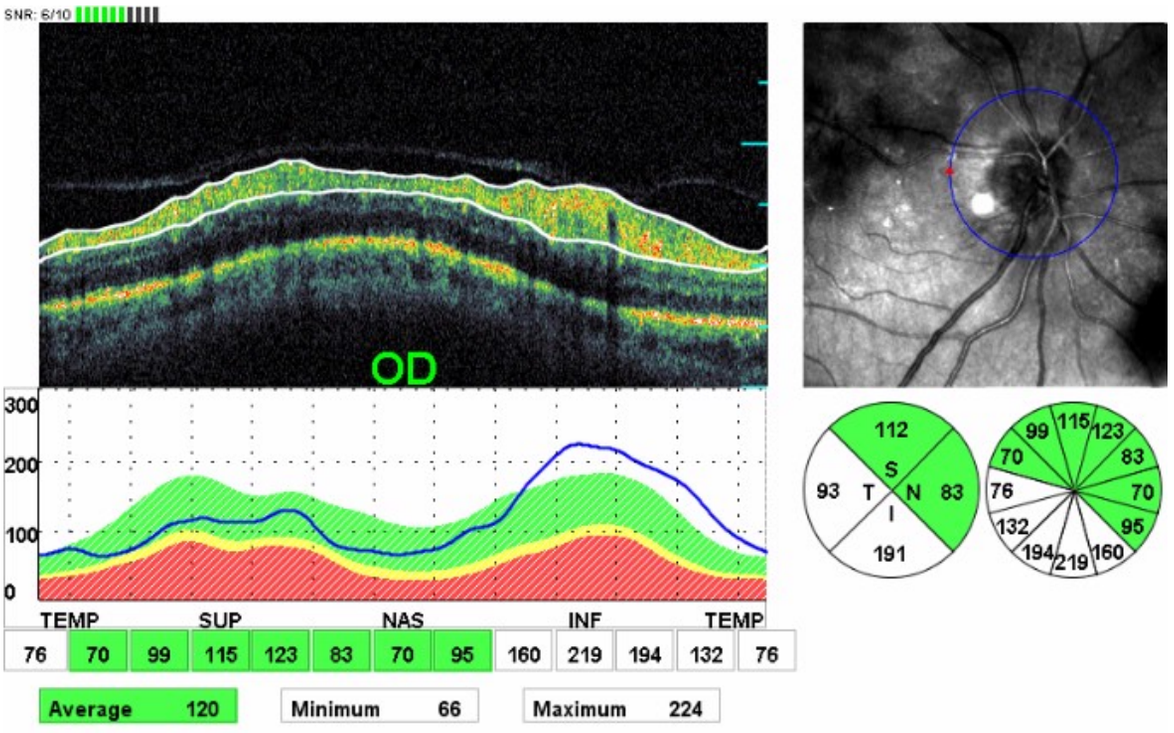

Figure 20. RNFL swelling in a patient with NA-AION 4 weeks following presentation.

glaucoma eyes. For the same level of MD, open angle glaucoma eyes had larger cup area, smaller rim area, larger cup/disc ratio, larger cup volume, smaller rim volume, and greater cup depth. When comparing the two types of AION, the non-arteritic type had smaller cup area, a larger rim area, and a smaller cup/disc ratio (61). In order to explain the discrepancy in the morphology of the optic nerve damage between both types of AION and glaucoma the authors suggest that glaucoma affects laminar connective tissue more than the prelaminar structures (as opposed to AION) and this causes the development of larger and deeper cups in glaucoma. The loss of laminar connective tissue leads in turn to retrodisplacement and thinning of the lamina cribrosa which causes the larger cup size in glaucoma. Both glaucoma and AION cause retinal gagglion cell loss but AION does not affect the laminar tissues.

9.4. Leber's Hereditary Optic Neuropathy (LHON)

LHON is a rare mitochondrial disorder that affects males and is associated with mutations of the maternal mitochondrial DNA. It presents with acute loss of vision between the ages 10 – 60 but most often in the age range 15-35. Early signs are optic disc hyperaemia and nerve fiber swelling. In the later stages optic atrophy dominates the clinical picture. Differential diagnosis is as in papilledema.

OCT demonstrated statistically significant increase of the RNFL thickness (mean, superior, inferior, nasal) in the early stage of the disease (6-8 weeks after initial presentation). Nine months after onset there is a decrease in RNFL thickness in all but nasal quadrants (108,109).

http://dx.doi.org/10.5772/55157

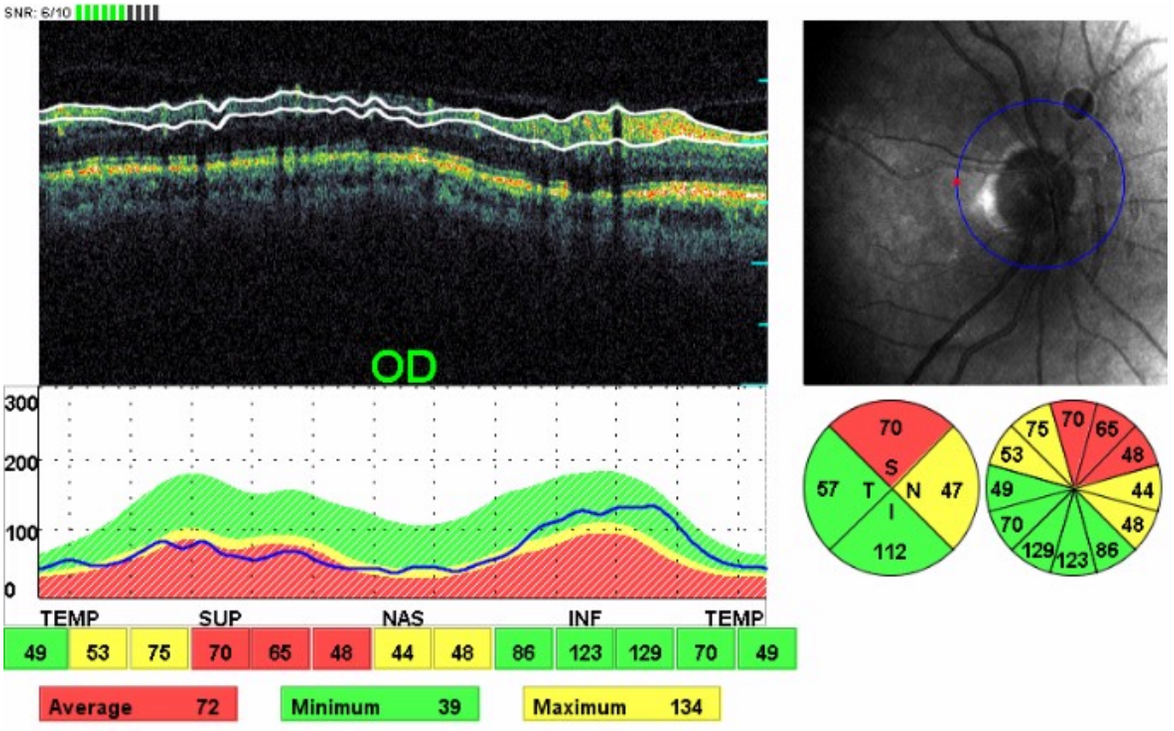

Figure 21. Same patient as in fig 20 3 months after initial presentation of NA-AION. Swelling of the RHFL has subsided and atrophy has begun to set in.

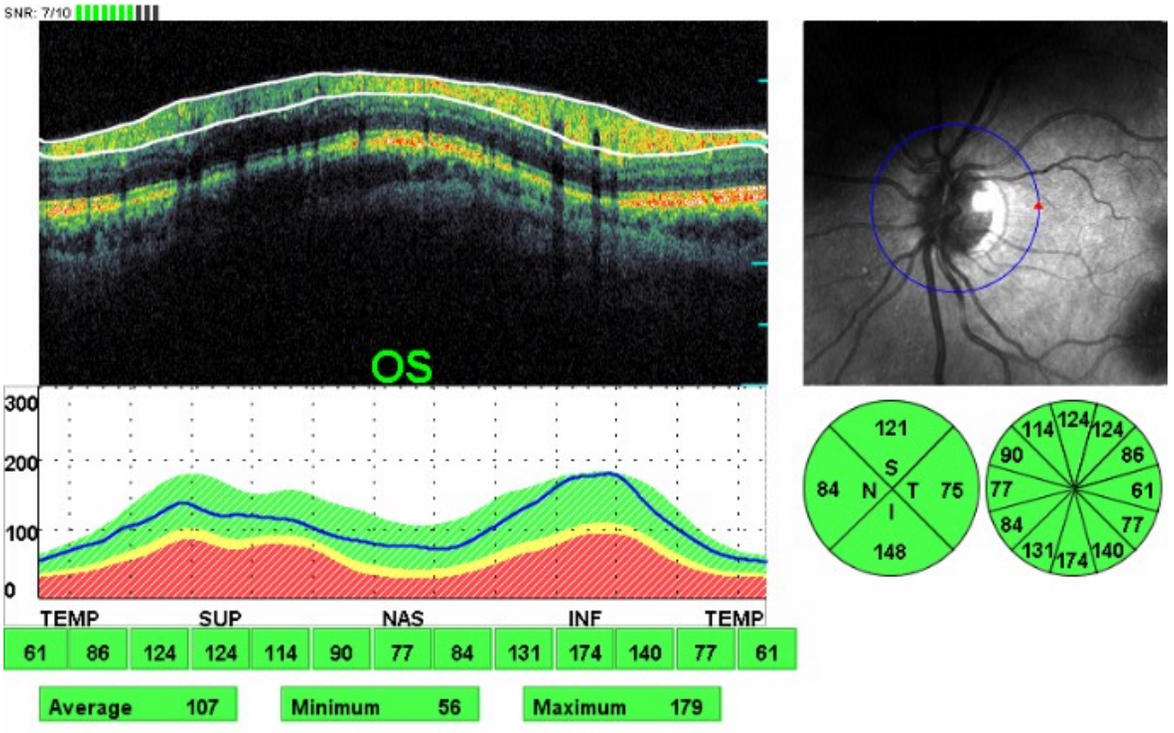

Figure 22. Fellow eye of the same patient as in fig 10 showing a crowded disc.

Unaffected male carriers had higher RNFL thickness in the temporal and inferior quadrants which was more pronounced in those with the 11778 mutation. Unaffected female carriers had a RNFL thickness increase in the temporal quadrant more pronounced in those with the 11778 mutation (110). Patients with the 11778 mutation tend to have increased RNFL thickness in the early stages of the disease and decreased thickness in the later stages compared to those with the 14484 mutation (111).

9.5. Optic atrophy

Optic atrophy is classified aetiologically as:

Primary (not associated with previous optic disc swelling. Most common causes are compressive lesions of the optic pathways up to the lateral geniculate bodies, hereditary disorders and multiple sclerosis).

Secondary (following longstanding swelling of the optic nerve head (papilledema, AION, papillitis)

Consecutive (following retinal diseases with widespread destruction of the retina such as retinitis pigmentosa, central retinal artery occlusion, vasculitis)

The new devices for the analysis of RNFL have been employed for the differential diagnosis of those types of optic atrophy in which the features of glaucomatous versus non-glaucomatous optic nerve damage are not clear. Autosomal dominant optic atrophy (ADOA, Kjer's optic neuropathy) is a rare hereditary disorder [it affects 1:35,000 people in the general population (112)] that can be misdiagnosed for normal tension glaucoma (113) and in this cases OCT provide useful information in order to reach the correct diagnosis. Several reports have shown that eyes with ADOA have reduced mean RNFL thickness and the quadrant most commonly affected being the temporal one (114-117). In contrast the glaucomatous process typically affects the inferior and superior sectors (118). There is also a reduction in macular thickness in patients with ADOA (119). Barboni et al (120) reported that the optic nerve heads in patients with ADOA have smaller size compared to normal controls.

Chiasmal compressive lesions produce a characteristic bitemporal hemianopia which is due to the preservation of the uncrossed fibers that originate from the temporal retina and enter the optic disc with the superior and inferior arcuate bands. The main damage therefore occurs in the nasal and temporal sectors of the disc and causes a characteristic ophthalmoscopic appearance named band atrophy. OCT has shown that not only the nasal and temporal sectors of the RNFL are affected but also the superior and inferior ones (121-123). OCT analysis of the optic nerve head could depict better than the Heidelberg Retina Tomograph the rim loss and subsequently the increased cup area in eyes with band atrophy (124).

Summary box

The new imaging modalities of the optic nerve head and RNFL thickness can describe with high accuracy the morphology of the above structures. However none of them has 100% accuracy in the diagnosis of glaucoma. RNFL thickness analysis seems to perform better than

optic disc analysis. Clinical examination is of utmost importance before reaching the diagnosis of glaucomatous optic neuropathy

Acknowledgements

The authors have no proprietary interest in any of the products mentioned in the manuscript

Author details

Vassilis Kozobolis, Aristeidis Konstantinidis* and Georgios Labiris

*Address all correspondence to: aristeidiskon@hotmail.com

Eye Department, University Hospital of Alexandroupolis, Alexandroupolis, Greece

References

[1] Piette, S. D, & Sergott, R. C. Pathological optic-disc cupping.Curr Opin Ophthalmol. (2006). Feb;, 17(1), 1-6.

[2] Airaksinen, P. J, Drance, S. M, Douglas, G. R, Mawson, D. K, & Nieminen, H. Diffuse and localized nerve fiber loss in glaucoma. Am J Ophthalmol. (1984). Nov;, 98(5), 566-71.

[3] Airaksinen, P. J, & Nieminen, H. Retinal nerve fiber layer photography in glaucoma. Ophthalmolog (1985). , 92, 877-879.

[4] Badalà, F, Nouri-mahdavi, K, Raoof, D. A, Leeprechanon, N, Law, S. K, & Caprioli, J. Optic disk and nerve fiber layer imaging to detect glaucoma. Am J Ophthalmol. (2007). Nov;, 144(5), 724-32.

[5] Zangwill, L. M, Williams, J, Berry, C. C, Knauer, S, & Weinreb, R. N. A comparison of optical coherence tomography and retinal nerve fiber layer photography for detection of nerve fiber layer damage in glaucoma. Ophthalmology. (2000). Jul;, 107(7), 1309-15.

[6] Deleón-ortega, J. E, & Arthur, S. N. McGwin G Jr, Xie A, Monheit BE, Girkin CA. Discrimination between glaucomatous and nonglaucomatous eyes using quantitative imaging devices and subjective optic nerve head assessment. Invest Ophthalmol Vis Sci. (2006). Aug;, 47(8), 3374-80.

[7] Greaney, M. J, Hoffman, D. C, Garway-heath, D. F, Nakla, M, Coleman, A. L, & Caprioli, J. Comparison of optic nerve imaging methods to distinguish normal eyes from those with glaucoma. Invest Ophthalmol Vis Sci. (2002). Jan;, 43(1), 140-5.

[8] Gianmarco VizzeriSara M Kjaergaard, Harsha L Rao, Linda M Zangwill. Role of imaging in glaucoma diagnosis and follow-up. Indian J Ophthalmol. (2011). January; 59(Suppl1): SS68., 59.

[9] Bowd, C, Weinreb, R. N, Lee, B, Emdadi, A, & Zangwill, L. M. Optic disk topography after medical treatment to reduce intraocular pressure. Am J Ophthalmol. (2000). Sep;, 130(3), 280-6.

[10] Townsend, K. A, Wollstein, G, & Schuman, J. S. Imaging of the retinal nerve fibre layer for glaucoma. Br J Ophthalmol. (2009). Feb;, 93(2), 139-43.

[11] Yanagisawa, M, Tomidokoro, A, Saito, H, Mayama, C, Aihara, M, Tomita, G, Shoji, N, & Araie, M. Atypical retardation pattern in measurements of scanning laser polarimetry and its relating factors. Eye (Lond). (2009). Sep;, 23(9), 1796-801.

[12] Da Pozzo SMarchesan R, Canziani T, Vattovani O, Ravalico G. Atypical pattern of retardation on GDx-VCC and its effect on retinal nerve fibre layer evaluation in glaucomatous eyes. Eye (Lond). (2006). Jul;, 20(7), 769-75.

[13] Mesiwala, N. K, Pekmezci, M, Huang, J. Y, Porco, T. C, & Lin, S. C. Comparison of Optic Disc Parameters Measured by RTVue-100 FDOCT Versus HRT-II. J Glaucoma. (2011). Jun 22.

[14] Leite, M. T, Rao, H. L, Zangwill, L. M, Weinreb, R. N, & Medeiros, F. A. Comparison of the diagnostic accuracies of the Spectralis, Cirrus, and RTVue optical coherence tomography devices in glaucoma. Ophthalmology.(2011). Jul;, 118(7), 1334-9.

[15] Leung, C. K, Chiu, V, Weinreb, R. N, Liu, S, Ye, C, Yu, M, Cheung, C. Y, Lai, G, & Lam, D. S. Evaluation of retinal nerve fiber layer progression in glaucoma: a comparison between spectral-domain and time-domain optical coherence tomography. Ophthalmology.(2011). Aug;, 118(8), 1558-62.

[16] Leung, C. K, Cheung, C. Y, Weinreb, R. N, Qiu, Q, Liu, S, Li, H, Xu, G, Fan, N, Huang, L, Pang, C. P, & Lam, D. S. Retinal nerve fiber layer imaging with spectral-domain optical coherence tomography: a variability and diagnostic performance study. Ophthalmology. (2009). Jul;e1-2., 116(7), 1257-63.

[17] Lee, S, Sung, K. R, Cho, J. W, Cheon, M. H, Kang, S. Y, & Kook, M. S. Spectral-domain optical coherence tomography and scanning laser polarimetry in glaucoma diagnosis. Jpn J Ophthalmol. (2010). Nov;, 54(6), 544-9.

[18] Garudadri, C. S, Rao, H. L, Parikh, R. S, Jonnadula, G. B, Selvaraj, P, Nutheti, R, & Thomas, R. Effect of optic disc size and disease severity on the diagnostic capability of glaucomaimaging technologies in an Indian population. J Glaucoma. (2012). Sep;, 21(7), 475-80.

[19] Oddone, F, Centofanti, M, Tanga, L, Parravano, M, Michelessi, M, Schiavone, M, Villani, C. M, Fogagnolo, P, & Manni, G. Influence of disc size on optic nerve head versus retinal nerve fiber layer assessment for diagnosing glaucoma. Ophthalmology. (2011). Jul;, 118(7), 1340-7.

[20] Medeiros, F. A, Zangwill, L. M, Bowd, C, Sample, P. A, & Weinreb, R. N. Influence of disease severity and optic disc size on the diagnostic performance of imaging instruments in glaucoma. Invest Ophthalmol Vis Sci. (2006). Mar;, 47(3), 1008-15.

[21] Leite, M. T, Zangwill, L. M, Weinreb, R. N, Rao, H. L, Alencar, L. M, Sample, P. A, & Medeiros, F. A. Effect of disease severity on the performance of Cirrus spectral-domain OCT for glaucoma diagnosis. Invest Ophthalmol Vis Sci. (2010). Aug;, 51(8), 4104-9.

[22] Kanamori, A, Nagai-kusuhara, A, Escaño, M. F, Maeda, H, Nakamura, M, & Negi, A. Comparison of confocal scanning laser ophthalmoscopy, scanning laser polarimetry and optical coherence tomography to discriminate ocular hypertension and glaucoma at an early stage. Graefes Arch Clin Exp Ophthalmol. (2006). Jan;, 244(1), 58-68.

[23] Leung, C. K, Ye, C, Weinreb, R. N, Cheung, C. Y, Qiu, Q, Liu, S, Xu, G, & Lam, D. S. Retinal nerve fiber layer imaging with spectral-domain optical coherence tomography a study on diagnostic agreement with Heidelberg Retinal Tomograph. Ophthalmology. (2010). Feb;, 117(2), 267-74.

[24] Medeiros, F. A, Vizzeri, G, Zangwill, L. M, Alencar, L. M, Sample, P. A, & Weinreb, R. N. Comparison of retinalnervefiberlayer and optic disc imaging for diagnosing glaucoma in patients suspected of having the disease. Ophthalmology. (2008). Aug;, 115(8), 1340-6.

[25] Alencar, L. M, Zangwill, L. M, Weinreb, R. N, Bowd, C, Sample, P. A, Girkin, C. A, Liebmann, J. M, & Medeiros, F. A. A comparison of rates of change in neuroretinal rim area and retinalnerve fiber layer thickness in progressive glaucoma. Invest Ophthalmol Vis Sci. (2010). Jul;, 51(7), 3531-9.

[26] Jonas, J. B, Budde, W. M, & Panda-jonas, S. Ophthalmoscopic evaluation of the optic nerve head. Surv Ophthalmol (1999).

[27] Oliveira, C, Harizman, N, Girkin, C. A, Xie, A, Tello, C, Liebmann, J. M, & Ritch, R. Axial length and optic disc size in normal eyes.Br J Ophthalmol. (2007). Jan;, 91(1), 37-9.

[28] Samarawickrama, C, Hong, T, Jonas, J. B, & Mitchell, P. Measurement of normal optic nerve headparameters.Surv Ophthalmol. (2012). Jul-Aug;, 57(4), 317-36.

[29] Jonas, J. B. Optic disk size correlated with refractive error. Am J Ophthalmol. (2005). Feb;, 139(2), 346-8.

[30] Jonas, J. B, Gusek, G. C, Guggenmoos-holzmann, I, & Naumann, G. O. Variability of the real dimensions of normal human optic discs.Graefes Arch Clin Exp Ophthalmol. (1988). , 226(4), 332-6.

[31] Jonas, J. B, Gusek, G. C, & Naumann, G. O. Optic disc, cup and neuroretinal rim size, configuration and correlations in normal eyes.Invest Ophthalmol Vis Sci. (1988). Jul;, 29(7), 1151-8.

[32] Crowston, J G, Hopley, C R, Healey, P R, Lee, A, & Mitchell, P. The effect of optic disc diameter on vertical cup to disc ratio percentiles in a population based cohort: the Blue Mountains Eye Study Br J Ophthalmol. (2004). June; , 88(6), 766-770.

[33] You, Q. S, Xu, L, & Jonas, J. B. Tilted optic discs: The Beijing Eye Study.Eye (Lond). (2008). May;, 22(5), 728-9.

[34] Jonas, J. B, Schmidt, A. M, Müller-bergh, J. A, Schlötzer-schrehardt, U. M, & Naumann, G. O. Human optic nerve fiber count and optic disc size.Invest Ophthalmol Vis Sci. (1992). May;, 33(6), 2012-8.

[35] Tuulonen, A, & Airaksinen, P. J. Optic disc size in exfoliative, primary open angle, and low-tension glaucoma. Arch Ophthalmol. (1992). Feb;, 110(2), 211-3.

[36] Jonas, J. B, & Papastathopoulos, K. I. Optic disk appearance in pseudoexfoliation syndrome. Am J Ophthalmol. (1997). Feb;, 123(2), 174-80.

[37] Schulzer, M, Drance, S. M, & Douglas, G. R. A comparison of treated and untreated-glaucomasuspects. Ophthalmology. (1991). Mar;, 98(3), 301-7.

[38] Cioffi, G. A, & Liebmann, J. M. Translating the OHTSresults into clinical practice.J Glaucoma. (2002). Oct;, 11(5), 375-7.

[39] Airaksinen, P. J, & Alanko, H. I. Effect of retinalnervefibreloss on the opticnervehead-configuration in earlyglaucoma. Graefes Arch Clin Exp Ophthalmol. (1983). , 220(4), 193-6.

[40] Quigley, H. A, Addicks, E. M, & Green, W. R. Optic nerve damage in human glaucoma. III. Quantitative correlation of nerve fiber loss and visual field defect in glaucoma, ischemic neuropathy, papilledema, and toxic neuropathy.Arch Ophthalmol. (1982). Jan;, 100(1), 135-46.

[41] Leung, C. K, Choi, N, Weinreb, R. N, Liu, S, Ye, C, Liu, L, Lai, G. W, Lau, J, & Lam, D. S. Retinal nerve fiber layer imaging with spectral-domain optical coherence tomography: pattern of RNFL defects in glaucoma. Ophthalmology. (2010). Dec;, 117(12), 2337-44.

[42] Takahashi, H, Goto, T, Shoji, T, Tanito, M, Park, M, & Chihara, E. Diabetes-associated retinal nerve fiber damage evaluated with scanning laser polarimetry. Am J Ophthalmol. (2006). Jul;, 142(1), 88-94.

[43] Jonas, J. B, Budde, W. M, Németh, J, Gründler, A. E, Mistlberger, A, & Hayler, J. K. Centralretinal vessel trunkexit and location of glaucomatous parapapillary atrophy in glaucoma. Ophthalmology. (2001). Jun;, 108(6), 1059-64.

[44] Jonas, J. B, & Fernadez, M. C. Shape of the neuroretinal rim and position of the central retinal vessels in glaucoma. Br L Ophthalmol. (1994). , 99-102.

[45] Uhler, T. A, & Piltz-seymour, J. Optic disc hemorrhages in glaucoma and ocular hypertension: implications and recommendations.Curr Opin Ophthalmol. (2008). Mar;, 19(2), 89-94.

[46] Wang, Y, Xu, L, Hu, L, Wang, Y, Yang, H, & Jonas, J. B. Frequency of optic diskhemorrhages in adult chinese in rural and urban china: the Beijing eye study. Am J Ophthalmol. (2006). Aug;, 142(2), 241-6.

[47] Sonnsjö, B, Dokmo, Y, & Krakau, T. Disc haemorrhages, precursors of open angle glaucoma.Prog Retin Eye Res. (2002). Jan;, 21(1), 35-56.

[48] Yamamoto, T, Iwase, A, Kawase, K, Sawada, A, & Ishida, K. Optic disc hemorrhages detected in a large-scale eye disease screening project. J Glaucoma. (2004). Oct;, 13(5), 356-60.

[49] Healey, P. R, Mitchell, P, Smith, W, & Wang, J. J. Optic disc hemorrhages in a population with and without signs of glaucoma. Ophthalmology. (1998). Feb;, 105(2), 216-23.

[50] Wang, Y, Xu, L, Hu, L, Wang, Y, Yang, H, & Jonas, J. B. Frequency of optic disk hemorrhages in adult chinese in rural and urban china: the Beijing eye study. Am J Ophthalmol. (2006). Aug;, 142(2), 241-6.

[51] Tomidokoro, A, Iwase, A, Araie, M, Yamamoto, T, & Kitazawa, Y. Population-based prevalence of optic disc haemorrhages in elderly Japanese. Eye (Lond). (2009). May;, 23(5), 1032-7.

[52] Park, K. H, Tomita, G, Liou, S. Y, & Kitazawa, Y. Correlation between peripapillaratrophy and optic nerve damage in normal-tension glaucoma.Ophthalmology. (1996). Nov;, 103(11), 1899-906.

[53] Uhm, K. B, Lee, D. Y, Kim, J. T, & Hong, C. Peripapillaryatrophy in normal and primary open-angle glaucoma. Korean J Ophthalmol. (1998). Jun;, 12(1), 37-50.

[54] Xu, L, Wang, Y, Yang, H, & Jonas, J. B. Differences in parapapillary atrophy between glaucomatous and normal eyes: the Beijing Eye Study. Am J Ophthalmol. (2007). Oct;, 144(4), 541-6.

[55] Uchida, H, Ugurlu, S, & Caprioli, J. Increasing peripapillary atrophy is associated with progressive glaucoma.Ophthalmology. (1998). Aug;, 105(8), 1541-5.

[56] See, J. L, Nicolela, M. T, & Chauhan, B. C. Rates of neuroretinal rim and peripapillaryatrophy area change: a comparative study of glaucoma patients and normal controls. Ophthalmology. (2009). May;, 116(5), 840-7.

[57] Ahn, J. K, Kang, J. H, & Park, K. H. Correlation between a disc hemorrhage and peripapillaryatrophy in glaucoma patients with a unilateral disc hemorrhage. J Glaucoma. (2004). Feb;, 13(1), 9-14.

[58] Roodhooft, J. M. Nonglaucomatous optic disk atrophy and excavation in the elderly.Bull Soc Belge Ophtalmol. (2003).

[59] Fournier, A. V, Damji, K. F, Epstein, D. L, & Pollock, S. C. Discexcavation in dominant optic atrophy: differentiation from normal tension glaucoma.Ophthalmology. (2001). Sep;, 108(9), 1595-602.

[60] Trobe, J. D, Glaser, J. S, Cassady, J, Herschler, J, & Anderson, D. R. Nonglaucomatous excavation of the optic disc. Arch Ophthalmol. (1980). Jun;, 98(6), 1046-50.

[61] Danesh-meyer, H. V, Boland, M. V, Savino, P. J, Miller, N. R, Subramanian, P. S, Girkin, C. A, & Quigley, H. A. Optic disc morphology in open-angle glaucoma compared with anterior ischemic optic neuropathies. Invest Ophthalmol Vis Sci. (2010). Apr;, 51(4), 2003-10.

[62] Jonas, J. B. Clinical implications of peripapillary atrophy in glaucoma. Curr Opin Ophthalmol. (2005). Apr;, 16(2), 84-8.

[63] You, Q. S, Xu, L, & Jonas, J. B. Tilted optic discs: The Beijing Eye Study.Eye (Lond). (2008). May;, 22(5), 728-9.

[64] Hwang, Y. H, Yoo, C, & Kim, Y. Y. Myopic optic disc tilt and the characteristics of peripapillary retinal nerve fiber layer thickness measured by spectral-domain optical coherence tomography. J Glaucoma. (2012). Apr-May;, 21(4), 260-5.

[65] Moschos, M. M, Triglianos, A, Rotsos, T, Papadimitriou, S, Margetis, I, Minogiannis, P, & Moschos, M. Tilted disc syndrome: an OCT and mfERG study. Doc Ophthalmol. (2009). Aug;, 119(1), 23-8.

[66] Gass, J. D. Serous detachment of the macula secondary to congenital pit of the optic nerve head. Am J Ophthalmol (1969). , 67, 821-841.

[67] Nduaguba, C, Ugurlu, S, & Caprioli, J. Acquiredpits of the optic nerve in glaucoma: prevalence and associated visual field loss. Acta Ophthalmol Scand. (1998). Jun;, 76(3), 273-7.

[68] Ohno-matsui, K, Akiba, M, Moriyama, M, Shimada, N, Ishibashi, T, Tokoro, T, & Spaide, R. F. Acquiredopticnerve and peripapillarypits in pathologicmyopia. Ophthalmology. (2012). Aug;, 119(8), 1685-92.

[69] Healey, P. R, & Mitchell, P. The prevalence of opticdiscpits and their relationship to glaucoma. J Glaucoma. (2008). Jan-Feb;, 17(1), 11-4.

[70] Ugurlu, S, Weitzman, M, Nduaguba, C, & Caprioli, J. Acquired pit of the optic nerve: a risk factor for progression of glaucoma. Am J Ophthalmol. (1998). Apr;, 125(4), 457-64.

[71] Srinivasan, G, Venkatesh, P, & Garg, S. Optical coherence tomographic characteristics in morning glory disc anomaly. Can J Ophthalmol. (2007). Apr;, 42(2), 307-9.

[72] Islam, N, Best, J, Mehta, J. S, Sivakumar, S, Plant, G. T, & Hoyt, W. F. Optic disc duplication or coloboma? Br J Ophthalmol. (2005). Jan;, 89(1), 26-9.

[73] Auw-haedrich, C, Staubach, F, & Witchel, H. Optic disk drusen. Surv Ophthalmol (2001). , 47, 515-532.

[74] Lee, K. M, Woo, S. J, & Hwang, J. M. Differentiation of optic nerve head drusen and optic disc edema with spectral-domain optical coherence tomography.Ophthalmology. (2011). May;, 118(5), 971-7.

[75] Wester, S. T, Fantes, F. E, Lam, B. L, Anderson, D. R, Mcsoley, J. J, & Knighton, R. W. Characteristics of optic nerve head drusen on optical coherence tomography images. Ophthalmic Surg Lasers Imaging. (2010). Jan-Feb;, 41(1), 83-90.

[76] Hayashi, K, Tomidokoro, A, Konno, S, Mayama, C, Aihara, M, & Araie, M. Evaluation of optic nerve head configurations of superior segmental optic hypoplasia by spectral-domain optical coherence tomography. Br J Ophthalmol. (2010). Jun;, 94(6), 768-72.

[77] Lee, H. J, & Kee, C. Optical coherence tomography and Heidelberg retina tomography for superior segmental optic hypoplasia. Br J Ophthalmol. (2009). Nov;, 93(11), 1468-73.

[78] Vartin, C V, Nguyen, A. M, Balmitgere, T, Bernard, M, Tilikete, C, & Vighetto, A. Detection of mild papilloedema using spectral domain optical coherence tomography.Br J Ophthalmol. (2012). Mar;, 96(3), 375-9.

[79] Skau, M, Milea, D, Sander, B, Wegener, M, & Jensen, R. OCT for optic disc evaluation in idiopathic intracranial hypertension. Graefes Arch Clin Exp Ophthalmol. (2011). May;, 249(5), 723-30.

[80] Rebolleda, G, & Muñoz-negrete, F. J. Follow-up of mild papilledema in idiopathic intracranial hypertension with optical coherence tomography. Invest Ophthalmol Vis Sci. (2009). Nov;, 50(11), 5197-200.

[81] Kupersmith, M. J, Kardon, R, Durbin, M, Horne, M, & Shulman, J. Scanning laser polarimetry reveals status of RNFL integrity in eyes with optic nerve head swelling by OCT. Invest Ophthalmol Vis Sci. (2012). Apr 18;, 53(4), 1962-70.

[82] Kupersmith, M. J, Sibony, P, Mandel, G, Durbin, M, & Kardon, R. H. Optical coherence tomography of the swollen optic nerve head: deformation of the peripapillary retinal pigment epithelium layer in papilledema. Invest Ophthalmol Vis Sci.(2011). Aug 22;, 52(9), 6558-64.

[83] Sibony, P, Kupersmith, M. J, & Rohlf, F. J. Shape analysis of the peripapillary RPE layer in papilledema and ischemic optic neuropathy. Invest Ophthalmol Vis Sci.(2011). Oct 10;, 52(11), 7987-95.

[84] Parisi, V, Manni, G, Spadaro, M, Colacino, G, Restuccia, R, Marchi, S, Bucci, M. G, & Pierelli, F. Correlation between morphological and functional retinal impairment in multiple sclerosis patients. Invest Ophthalmol Vis Sci. (1999). Oct; , 40(11), 2520-7.

[85] Trip, S. A, Schlottmann, P. G, Jones, S. J, Altmann, D. R, Garway-heath, D. F, Thompson, A. J, Plant, G. T, & Miller, D. H. Retinal nerve fiber layer axonal loss and visual dysfunction in optic neuritis. Ann Neurol. (2005). Sep; , 58(3), 383-91.

[86] Noval, S, Contreras, I, Rebolleda, G, & Muñoz-negrete, F. J. Optical coherence tomography versus automated perimetry for follow-up of optic neuritis. Acta Ophthalmol Scand. (2006). Dec; , 84(6), 790-4.

[87] Pro, M. J, Pons, M. E, Liebmann, J. M, Ritch, R, Zafar, S, Lefton, D, & Kupersmith, M. J. Imaging of the optic disc and retinal nerve fiber layer in acute optic neuritis. J Neurol Sci. (2006). Dec 1; 250(1-2):114-9.

[88] Costello, F, Coupland, S, Hodge, W, Lorello, G. R, Koroluk, J, Pan, Y. I, Freedman, M. S, Zackon, D. H, & Kardon, R. H. Quantifying axonal loss after optic neuritis with optical coherence tomography. Ann Neurol. (2006). Jun; , 59(6), 963-9.

[89] Costello, F, Hodge, W, Pan, Y. I, Eggenberger, E, Coupland, S, & Kardon, R. H. Tracking retinal nerve fiber layer loss after optic neuritis: a prospective study using optical coherence tomography. Mult Scler. (2008). Aug; , 14(7), 893-905.

[90] Costello, F, Hodge, W, Pan, Y. I, Freedman, M, & Demeulemeester, C. Differences in retinal nerve fiber layer atrophy between multiple sclerosis subtypes. J Neurol Sci. (2009). Jun 15; 281(1-2):74-9.

[91] Fisher, J. B, Jacobs, D. A, Markowitz, C. E, Galetta, S. L, Volpe, N. J, Nano-schiavi, M. L, Baier, M. L, Frohman, E. M, Winslow, H, Frohman, T. C, Calabresi, P. A, Maguire, M. G, Cutter, G. R, & Balcer, L. J. Relation of visual function to retinal nerve fiber layer thickness in multiple sclerosis. Ophthalmology. (2006). Feb; , 113(2), 324-32.

[92] Henderson, A. P, Trip, S. A, Schlottmann, P. G, Altmann, D. R, Garway-heath, D. F, Plant, G. T, & Miller, D. H. An investigation of the retinal nerve fibre layer in progressive multiple sclerosis using optical coherence tomography. Brain. (2008). Jan; 131(Pt 1): 277-87.

[93] Pueyo, V, Martin, J, Fernandez, J, Almarcegui, C, Ara, J, Egea, C, Pablo, L, & Honrubia, F. Axonal loss in the retinal nerve fiber layer in patients with multiple sclerosis. Mult Scler. (2008). Jun; , 14(5), 609-14.

[94] Pulicken, M, Gordon-lipkin, E, Balcer, L. J, Frohman, E, Cutter, G, & Calabresi, P. A. Optical coherence tomography and disease subtype in multiple sclerosis. Neurology. (2007). Nov 27; , 69(22), 2085-92.

[95] Sepulcre, J, Murie-fernandez, M, Salinas-alaman, A, García-layana, A, Bejarano, B, & Villoslada, P. Diagnostic accuracy of retinal abnormalities in predicting disease activity in MS.Neurology. (2007). May 1; , 68(18), 1488-94.

[96] Toledo, J, Sepulcre, J, Salinas-alaman, A, García-layana, A, Murie-fernandez, M, Bejarano, B, & Villoslada, P. Retinal nerve fiber layer atrophy is associated with physical and cognitive disability in multiple sclerosis. Mult Scler. (2008). Aug; , 14(7), 906-12.

[97] Spain, R. I, Maltenfort, M, Sergott, R. C, & Leist, T. P. Thickness of retinal nerve fiber layer correlates with disease duration in parallel with corticospinal tract dysfunction in untreated multiple sclerosis. J Rehabil Res Dev. (2009). , 46(5), 633-42.

[98] Costello, F, Hodge, W, Pan, Y. I, & Metz, L. Kardon RH Retinal nerve fiber layer and future risk of multiple sclerosis. Can J Neurol Sci. (2008). Sep; , 35(4), 482-7.

[99] Bertuzzi, F, Suzani, M, Tagliabue, E, Cavaletti, G, Angeli, R, Balgera, R, Rulli, E, Ferrarese, C, & Miglior, S. Diagnostic validity of optic disc and retinal nerve fiber layer

evaluations in detecting structural changes after optic neuritis. Ophthalmology. (2010). Jun;, 117(6), 1256-1264.

[100] Savini, G, Bellusci, C, Carbonelli, M, Zanini, M, Carelli, V, Sadun, A. A, & Barboni, P. Detection and quantification of retinal nerve fiber layer thickness in optic disc edema using stratus OCT. Arch Ophthalmol. (2006). Aug;, 124(8), 1111-7.

[101] Alasil, T, Tan, O, Lu, A. T, Huang, D, & Sadun, A. A. Correlation of Fourier domain optical coherence tomography retinal nerve fiber layer maps with visual fields in nonarteritic ischemic optic neuropathy. Ophthalmic Surg Lasers Imaging. (2008). Jul-Aug;39(4 Suppl):S, 71-9.

[102] Contreras, I, Noval, S, Rebolleda, G, & Muñoz-negrete, F. J. Follow-up of nonarteritic anterior ischemic optic neuropathy with optical coherence tomography. Ophthalmology. (2007). Dec;, 114(12), 2338-44.

[103] Bellusci, C, Savini, G, Carbonelli, M, Carelli, V, Sadun, A. A, & Barboni, P. Retinal nerve fiber layer thickness in nonarteritic anterior ischemic optic neuropathy: OCT characterization of the acute and resolving phases. Graefes Arch Clin Exp Ophthalmol. (2008). May;, 246(5), 641-7.

[104] Aggarwal, D, Tan, O, Huang, D, & Sadun, A. A. Patterns of ganglion cell complex and nerve fiber layer loss in nonarteritic ischemic optic neuropathy by Fourier-domain optical coherence tomography. Invest Ophthalmol Vis Sci. (2012). Jul 3;, 53(8), 4539-45.

[105] Deleón-ortega, J, Carroll, K. E, Arthur, S. N, & Girkin, C. A. Correlations between retinal nerve fiber layer and visual field in eyes with nonarteritic anterior ischemic optic neuropathy. Am J Ophthalmol. (2007). Feb;, 143(2), 288-294.

[106] Papchenko, T, Grainger, B. T, Savino, P. J, Gamble, G. D, & Danesh-meyer, H. V. Macular thickness predictive of visual field sensitivity in ischaemic optic neuropathy. Acta Ophthalmol. (2012). Sep;90(6):e, 463-9.

[107] Horowitz, J, Fishelzon-arev, T, Rath, E. Z, Segev, E, & Geyer, O. Comparison of optic nerve head topography findings in eyes with non-arteritic anterior ischemic optic neuropathy and eyes with glaucoma. Graefes Arch Clin Exp Ophthalmol. (2010). Jun;, 248(6), 845-51.

[108] Barboni, P, Carbonelli, M, & Savini, G. Ramos Cdo V, Carta A, Berezovsky A, Salomao SR, Carelli V, Sadun AA. Natural history of Leber's hereditary optic neuropathy: longitudinal analysis of the retinal nerve fiber layer by optical coherence tomography. Ophthalmology. (2010). Mar;, 117(3), 623-7.

[109] Barboni, P, Savini, G, Valentino, M. L, Montagna, P, Cortelli, P, De Negri, A. M, Sadun, F, Bianchi, S, Longanesi, L, Zanini, M, De Vivo, A, & Carelli, V. Retinal nerve fiber layer evaluation by optical coherence tomography in Leber's hereditary optic neuropathy. Ophthalmology. (2005). Jan;, 112(1), 120-6.

[110] Savini, G, Barboni, P, Valentino, M. L, Montagna, P, Cortelli, P, De Negri, A. M, Sadun, F, Bianchi, S, Longanesi, L, Zanini, M, & Carelli, V. Retinal nerve fiber layer evaluation

by optical coherence tomography in unaffected carriers with Leber's hereditary optic neuropathy mutations.Ophthalmology. (2005). Jan;, 112(1), 127-31.

[111] Seo, J. H, Hwang, J. M, & Park, S. S. Comparison of retinal nerve fibre layers between 11778 and 14484 mutations in Leber's hereditary optic neuropathy. Eye (Lond). (2010). Jan;, 24(1), 107-11.

[112] Yu-wai-man, P, Griffiths, P. G, Burke, A, Sellar, P. W, Clarke, M. P, Gnanaraj, L, Ahkine, D, Hudson, G, Czermin, B, Taylor, R. W, Horvath, R, & Chinnery, P. F. The prevalence and natural history of dominant optic atrophy due to OPA1 mutations. Ophthalmology. (2010). Aug;117(8):1538-46, 1546

[113] Fournier, A. V, Damji, K. F, Epstein, D. L, & Pollock, S. C. Discexcavation in dominant optic atrophy: differentiation from normal tension glaucoma.Ophthalmology(2001). Sep;, 108(9), 1595-602.

[114] Barboni, P, Savini, G, Parisi, V, & Carbonelli, M. La Morgia C, Maresca A, Sadun F, De Negri AM, Carta A, Sadun AA, Carelli V. Retinal nerve fiber layer thickness in dominant optic atrophy measurements by optical coherence tomography and correlation with age.Ophthalmology. (2011). Oct;, 118(10), 2076-80.

[115] Milea, D, Sander, B, Wegener, M, Jensen, H, Kjer, B, Jørgensen, T. M, Lund-andersen, H, & Larsen, M. Axonal loss occurs early in dominant optic atrophy. Acta Ophthalmol. (2010). May;, 88(3), 342-6.

[116] Kim, T. W, & Hwang, J. M. Stratus OCT in dominant optic atrophy: features differentiating it from glaucoma. J Glaucoma. (2007). Dec;, 16(8), 655-8.

[117] Yu-wai-man, P, Bailie, M, Atawan, A, Chinnery, P. F, & Griffiths, P. G. Pattern of retinal ganglion cell loss in dominant optic atrophy due to OPA1 mutations. Eye (Lond).(2011). May;, 25(5), 596-602.

[118] Bowd, C, Weinreb, R. N, Williams, J. M, et al. The retinal nerve fiber layer thickness in ocular hypertensive, normal, and glaucomatous eyes with optical coherence tomography. Arch Ophthalmol (2000). , 118, 22-6.

[119] Ito, Y, Nakamura, M, Yamakoshi, T, Lin, J, Yatsuya, H, & Terasaki, H. Reduction of inner retinal thickness in patients with autosomal dominant optic atrophy associated with OPA1 mutations. Invest Ophthalmol Vis Sci. (2007). Sep;, 48(9), 4079-86.

[120] Barboni, P, Carbonelli, M, Savini, G, Foscarini, B, Parisi, V, Valentino, M. L, Carta, A, De Negri, A, Sadun, F, Zeviani, M, Sadun, A. A, Schimpf, S, Wissinger, B, & Carelli, V. OPA1 mutations associated with dominant optic atrophy influence optic nerve head size. Ophthalmology. (2010). Aug;, 117(8), 1547-53.

[121] Monteiro, M L R, Leal, B C, Rosa, A A M, & Bronstein, M D. Optical coherence tomography analysis of axonal loss in band atrophy of the optic nerve. Br J Ophthalmol. (2004). July; , 88(7), 896-899.

[122] Kanamori, A, Nakamura, M, Matsui, N, Nagai, A, Nakanishi, Y, Kusuhara, S, Yamada, Y, & Negi, A. Optical coherence tomography detects characteristic retinal nerve fiber

layer thickness corresponding to band atrophy of the optic discs. Ophthalmology. (2004). Dec;, 111(12), 2278-83.

[123] Monteiro, M. L, Moura, F. C, & Medeiros, F. A. Diagnostic ability of optical coherence tomography with a normative database to detect band atrophy of the optic nerve. Am J Ophthalmol. (2007). May;, 143(5), 896-9.

[124] Nagai-kusuhara, A, Nakamura, M, Tatsumi, Y, Nakanishi, Y, & Negi, A. Disagreement between Heidelberg Retina Tomograph and optical coherence tomography in assessing optic nerve head configuration of eyes with band atrophy and normal eyes. Br J Ophthalmol. (2008). Oct;, 92(10), 1382-6.

IntechOpen